ARTICLES
https://doi.org/10.1038/s42255-019-0135-7
nature metabolism

Mechanism and effects of pulsatile GABA secretion from cytosolic pools in the human beta cell

Danusa Menegaz[1,16], D. Walker Hagan[2,16], Joana Almaça[1], Chiara Cianciaruso[3], Rayner Rodriguez-Diaz[1], Judith Molina[1], Robert M. Dolan[2], Matthew W. Becker[2], Petra C. Schwalie[3,4], Rita Nano[5], Fanny Lebreton[6], Chen Kang[7,8], Rajan Sah[7,8], Herbert Y. Gaisano[9], Per-Olof Berggren[10,11,12], Steinunn Baekkeskov[3,13]*, Alejandro Caicedo[1,10,14,15]* and Edward A. Phelps[2,3]*

Pancreatic beta cells synthesize and secrete the neurotransmitter GABA (γ-aminobutyric acid) as a paracrine and autocrine signal to help regulate hormone secretion and islet homeostasis. Islet GABA release has classically been described as a secretory-vesicle-mediated event. Yet, a limitation of the hypothesized vesicular GABA release from islets is the lack of expression of a vesicular GABA transporter in beta cells. Consequentially, GABA accumulates in the cytosol. Here, we provide evidence that the human beta cell effluxes GABA from a cytosolic pool in a pulsatile manner, imposing a synchronizing rhythm on pulsatile insulin secretion. The volume regulatory anion channel, functionally encoded by LRRC8A or Swell1, is critical for pulsatile GABA secretion. GABA content in beta cells is depleted and secretion is disrupted in islets from patients with type 1 and type 2 diabetes, suggesting that loss of GABA as a synchronizing signal for hormone output may correlate with diabetes pathogenesis.

The neurotransmitter GABA occurs at high concentrations in the inhibitory neurons of the central nervous system and the pancreatic islets of Langerhans[1]. The physiological purpose of GABA in islets was initially proposed to be a paracrine signal released from islet beta cells to inhibit alpha cells[2–4]. Recent evidence suggests that GABA also has strong protective and regenerative effects on the beta cells themselves[5]. GABA increases beta-cell mass in rodent and grafted human islets[6–11] and ameliorates diabetes in nonobese diabetic (NOD) mice[12]. Additionally, long-term GABA treatment in diabetic mice prevents alpha-cell hyperplasia[13] and promotes alpha-cell trans-differentiation into beta cells[14,15], although this latter effect is now disputed[16,17]. Immune cells possess receptors for GABA[18,19] which suppresses cytokine secretion, inhibits proliferation and tempers migration[10,18,20]. GABA inhibits autoreactive T-cell proliferation at the interstitial concentrations found in islets (0.1–10 μM)[21–23]. Together, this evidence implicates GABA as a potent trophic factor and suppressive immunomodulator in islets. It is conceivable that the loss of GABA may leave islet regions vulnerable to inflammation[20].

GABA is synthesized by the enzyme glutamic acid decarboxylase (GAD), which is expressed as two isoforms, GAD65 and GAD67. Human beta cells express only the GAD65 isoform[24], which is detected in the cytosol and anchored to the cytosolic face of Golgi and peripheral vesicle membranes by hydrophobic modifications including palmitoylations[1,25]. Earlier low-resolution imaging studies localized GAD and GABA to synaptic-like microvesicles in beta cells[26–28]. More recently, GABA has been detected in insulin granules from which it is released on stimulation with glucose to activate $GABA_A$ receptors in beta cells[29–32]. However, a substantial fraction of the GABA pool is independent of extracellular glucose concentration and yet contributes substantially to GABA signaling in the islet[31,33,34]. The source of this pool of GABA secretion appears to be the cytosol[35], but a mechanism linking cytosolic GABA to extracellular release has remained unidentified. In analogy to the role ambient GABA plays in the central nervous system[36], such release of GABA may be crucial for regulating islet cell excitability, coordinating cell activity throughout the islet and producing the beneficial effects mentioned above.

Here, we assessed how GABA is released from human beta cells. We compared GABA release from a predominantly cytosolic pool of intracellular GABA in beta cells with that of GABA contained in vesicular membrane compartments including synaptic-like microvesicles and the larger insulin secretory vesicles. We provide evidence that cytosolic GABA is released from human beta cells via volume regulatory anion channels (VRAC) in a pulsatile pattern that is independent of glucose concentration. Furthermore, the GABA-permissive taurine transporter (TauT) mediates uptake of interstitial GABA. Finally, we studied the impact of this nonvesicular

[1]Division of Endocrinology, Diabetes and Metabolism, Department of Medicine, University of Miami Miller School of Medicine, Miami, FL, USA. [2]J. Crayton Pruitt Family Department of Biomedical Engineering, University of Florida, Gainesville, FL, USA. [3]Institute of Bioengineering, School of Life Sciences, École Polytechnique Fédérale de Lausanne, Lausanne, Switzerland. [4]Swiss Institute of Bioinformatics, Lausanne, Switzerland. [5]Pancreatic Islet Processing Facility, Diabetes Research Institute, IRCCS San Raffaele Scientific Institute, Milan, Italy. [6]Cell Isolation and Transplantation Center, Faculty of Medicine, Department of Surgery, Geneva University Hospitals and University of Geneva, Geneva, Switzerland. [7]Center for Cardiovascular Research and Division of Cardiology, Department of Internal Medicine, Washington University School of Medicine, St Louis, MO, USA. [8]Department of Internal Medicine, Division of Cardiovascular Medicine, University of Iowa, Carver College of Medicine, Iowa City, IA, USA. [9]Department of Medicine, University of Toronto, Toronto, Ontario, Canada. [10]Diabetes Research Institute, University of Miami Miller School of Medicine, Miami, FL, USA. [11]The Rolf Luft Research Center for Diabetes & Endocrinology, Karolinska Institutet, Stockholm, Sweden. [12]Division of Integrative Biosciences and Biotechnology, WCU Program, University of Science and Technology, Pohang, Korea. [13]Departments of Medicine and Microbiology/Immunology, Diabetes Center, University of California San Francisco, San Francisco, CA, USA. [14]Department of Physiology and Biophysics, Miller School of Medicine, University of Miami, Miami, FL, USA. [15]Program in Neuroscience, Miller School of Medicine, University of Miami, Miami, FL, USA. [16]These authors contributed equally: Danusa Menegaz, D. Walker Hagan. *e-mail: sbaekkeskov@ucsf.edu; acaicedo@med.miami.edu; ephelps@bme.ufl.edu

GABA release on insulin secretion in human islets from nondiabetic and diabetic donors.

Results

Cytosolic pools of GABA are depleted in type 1 and type 2 diabetic islets. Earlier studies have shown that GABA is present at high levels in pancreatic islets[35,37], but due to the use of glutaraldehyde fixation, the resolution and the ability to use multiple antibody labeling of these early images were limited. Using an antibody that does not require glutaraldehyde fixation, we studied the GABA content in human islets from nondiabetic and diabetic donors. Human pancreas sections from nondiabetic donors immunostained for GABA, insulin and glucagon showed that GABA is highly concentrated in islets compared with the surrounding exocrine tissue (Fig. 1a). GABA staining was strongest in beta and delta cells, while alpha cells contained little or no GABA (Fig. 1a,b and Extended Data Fig. 1).

Comparing the GABA content in human pancreas sections from nondiabetic (Fig. 1c), type 2 diabetic (Fig. 1d) and type 1 diabetic (Fig. 1e,f) donors, we observed that type 1 and type 2 diabetic islets were depleted of GABA (Fig. 1g). In type 1 diabetic islets, the loss of GABA was not only observed in islets devoid of beta cells. Rather, even islets with residual beta cells were depleted of GABA (Fig. 1f). Taurine, a small molecule compound with molecular characteristics similar to GABA, was not depleted in diabetes, indicating that the loss of GABA is unlikely caused by varying sample quality or fixation (Extended Data Fig. 1). The loss of GABA in type 1 and type 2 diabetic islets observed by histology was confirmed by high-performance liquid chromatography (HPLC) measurements of the GABA content of isolated whole human islets from nondiabetic, type 1 diabetic and type 2 diabetic donors (Fig. 1h).

We next addressed whether the lack of GABA in beta cells from patients with type 2 and/or type 1 diabetes was the consequence of a loss of expression of the GABA-synthesizing enzyme GAD65 (Fig. 1i,j). GAD65 immunoreactivity in beta cells of patients with type 2 diabetes and in remaining beta cells in type 1 diabetes was similar to nondiabetic controls (Fig. 1k–n). Thus, the lack of GABA in diabetic islets is not due to lack of GAD65 expression in beta cells.

In human beta cells, GAD65 was highly expressed in Golgi membranes, peripheral vesicle membranes and the cytosol, while human alpha cells expressed GAD65 at low levels and the localization was restricted to endoplasmic reticulum (ER)/Golgi membranes while lacking in vesicle membranes and the cytosol (Extended Data Fig. 1). Remarkably, alpha cells contained little or no GABA (Fig. 1a,b) despite expressing GAD65. Expression of GAD65 in alpha cells of diabetic pancreases was indistinguishable from nondiabetic pancreases.

Subcellular localization suggests a nonvesicular GABA release mechanism in beta cells. Despites its well-established importance to islet physiology, the dominant mechanism of GABA release from islets remains unclear. We searched for immunohistochemical evidence of the canonical synaptic-like microvesicle mechanism of GABA release[27,28]. In GABA-ergic neurons, hydrophobic post-translational modifications of the synthesizing enzyme GAD65 anchor this protein to the cytosolic face of synaptic vesicle membranes where it colocalizes with the vesicular GABA transporter (VGAT)[38,39]. By association with GAD65, VGAT mediates transport of the product GABA into the synaptic vesicle lumen, where it accumulates in preparation for regulated secretion[40]. The existence of an analogous GABA-secreting system in islet cells would require co-expression of GAD65 and VGAT[41] or another as-yet unidentified vesicular GABA transporter in synaptic-like microvesicles. We found that almost all (>99%) human beta cells lacked expression of VGAT. VGAT expression was, however, detected in a small subset of human beta cells as well as in the somatostatin-producing delta cells, coinciding with the presence of GABA in vesicular compartments (Fig. 2a,b and Extended Data Fig. 2).

Human alpha cells were devoid of VGAT. In contrast, in rat islets, VGAT expression was mainly detected in alpha cells (Fig. 2b and Extended Data Fig. 2) while predominantly absent in beta and delta cells (Supplementary Table 1). VGAT, also known as the vesicular inhibitory amino acid transporter, is a transporter for glycine in addition to GABA in neurons[40] and in rat alpha cells, where it localizes with glycine in secretory vesicles[42]. The absence of GABA in rat alpha cells in our analyses is consistent with VGAT transporting glycine but not GABA in those cells and is in contrast with the results in human delta cells, which express VGAT and also contain GABA. A table summarizing the cell type-specific expression of GABA, GAD65 and VGAT in human and rat islets is included as supplementary information (Supplementary Table 1).

To assess whether VGAT is required for accumulation of GABA in peripheral vesicles, we compared the subcellular localization of GABA and GAD65 with synaptic vesicle markers synaptophysin, SV2C and VGAT in monolayers of human islet cells (Fig. 2c–i) and in hippocampal neurons (Fig. 2h,i and Extended Data Fig. 2). Almost all human beta cells (~99%) exhibited a uniform cytosolic staining pattern for GABA (Fig. 2c). However, in the rare VGAT$^+$

Fig. 1 | Cytosolic pools of GABA are depleted in type 1 and type 2 diabetic islets. a, A human pancreatic islet from a nondiabetic donor immunostained for GABA, insulin and glucagon. Image is representative of the dataset plotted in panel **b**. Scale bar, 50 µm. Right panels show higher magnification. Scale bar, 10 µm. **b**, Quantification of GABA colocalization with insulin ($n=15$ islets, 9 donors), glucagon ($n=15$ islets, 8 donors) and somatostatin ($n=15$ islets, 3 donors) in human islets. One-way ANOVA: insulin versus glucagon (*$P<0.0001$), insulin versus somatostatin (*$P=0.0182$). Center line indicates the mean. **c**–**f**, Human islets immunostained for GABA, insulin and glucagon from a nondiabetic (**c**), a type 2 diabetic (**d**), a type 1 diabetic (**e**) and a type 1 diabetic donor with residual beta-cell mass (**f**). Images are representative of the dataset plotted in panel **g**. Scale bars, 50 µm. **g**, Quantification of GABA mean fluorescence intensity (MFI) per human islet from nondiabetic ($n=15$ islets, 9 donors), type 1 diabetic ($n=15$ islets, 8 donors) and type 2 diabetic donors ($n=12$ islets, 8 donors). Background (BKGD) indicates average GABA MFI in acinar tissue outside of the islet. One-way ANOVA: ND versus T2D (*$P<0.0001$), ND versus T1D (*$P<0.0001$). Center line indicates the mean. **h**, HPLC quantification of GABA content for human islet preparations from nondiabetic ($n=8$ donors), type 2 diabetic ($n=3$ donors) and type 1 diabetic donors ($n=2$ donors). One-way ANOVA: ND versus T2D (*$P=0.0196$), ND versus T1D (*$P=0.0106$). Center line indicates the mean. **i**, Human islet from a nondiabetic donor immunostained for GAD65, insulin and glucagon. Image is representative of the dataset plotted in **j**. Scale bar, 50 µm. **j**, Quantification of GAD65 colocalization with insulin ($n=24$ islets, 9 donors), glucagon ($n=24$ islets, 9 donors) and somatostatin ($n=11$ islets, 3 donors) in human islets. One-way ANOVA: insulin versus glucagon (*$P<0.0001$), insulin versus somatostatin (*$P=0.0257$). Center line indicates the mean. **k**–**m**, Human islets immunostained for GAD65 from nondiabetic, type 2 diabetic and type 1 diabetic donors. Images are representative of the dataset plotted in panel **n**. Scale bars, 50 µm. **n**, Quantification of GAD65 MFI per human islet from nondiabetic ($n=23$ islets, 9 donors), type 1 diabetic ($n=23$, 8 donors) and type 2 diabetic donors ($n=24$ islets, 8 donors). BKGD indicates average GAD65 MFI in acinar tissue outside of the islet. One-way ANOVA: ND versus T2D (*$P=0.0380$), ND versus T1D (NS, $P=0.9511$), T2D versus T1D (NS, $P=0.0817$). Center line indicates the mean. Glcgn, glucagon; ND, nondiabetic; NS, not significant; Sst, somatostatin; T1D, type 1 diabetic; T2D, type 2 diabetic.

human beta cells (<1%; Fig. 2d) or in human delta cells (Fig. 2e), GABA exhibited a well-defined vesicular staining pattern that colocalized with VGAT. The VGAT$^+$/GABA$^+$ vesicular structures in beta cells colocalized with insulin, but not GAD65, identifying them as insulin secretory granules. The existence of a small population of VGAT$^+$ beta cells containing GABA in insulin granules reconciles our observations with previous reports of quantal exocytotic GABA release events that coincide with insulin release[31]. These data notwithstanding, the majority of beta cells did not express VGAT and had cytosolic rather than vesicular GABA content.

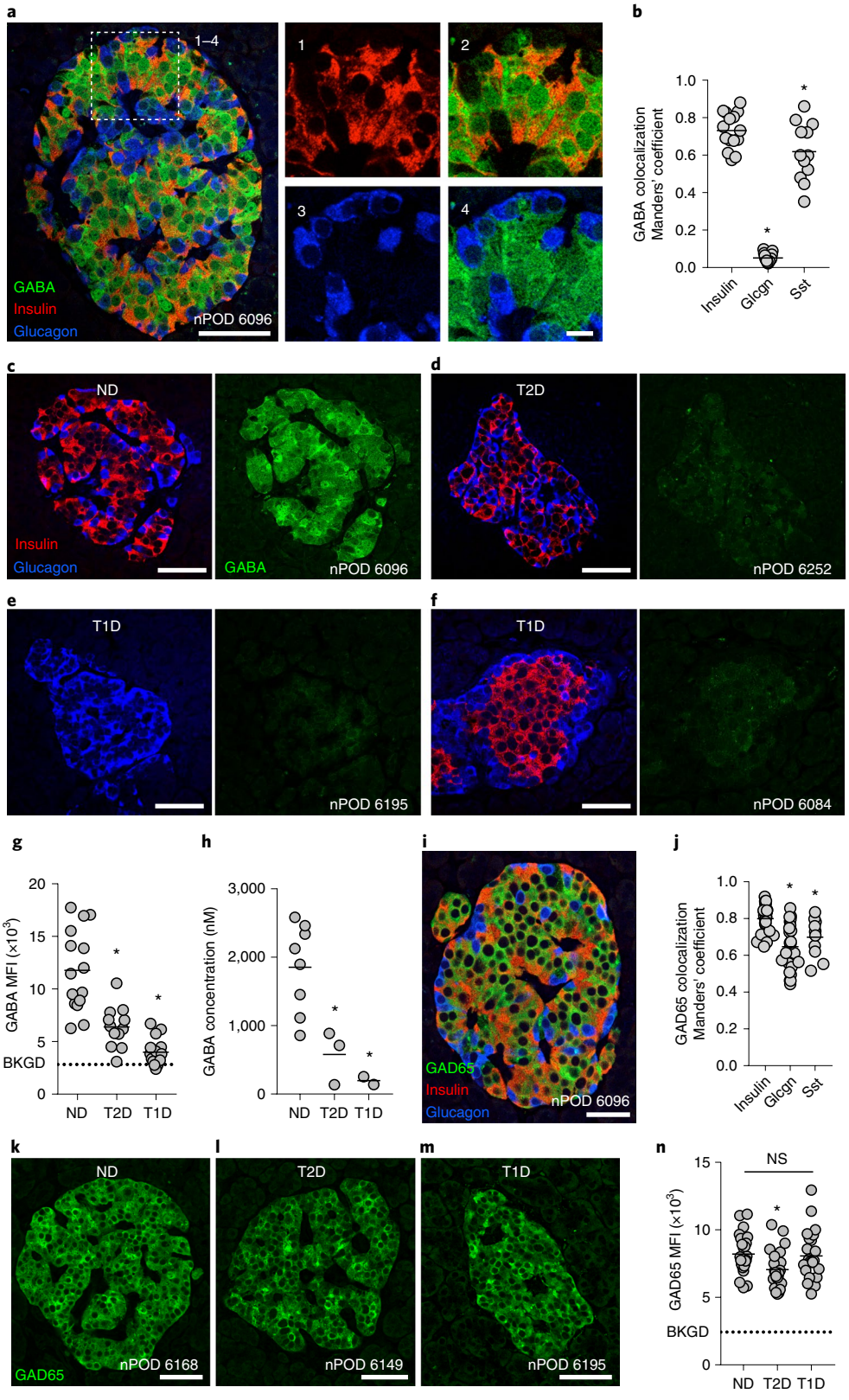

While GABA itself is mainly cytosolic, the GABA-synthesizing enzyme GAD65 exhibits a strongly punctate staining pattern in beta cells (Fig. 2f)[1]. These GAD65 puncta in beta cells have been previously described as synaptic-like microvesicles[27,28]. In human or rat beta cells containing predominantly cytosolic GABA, there was no concentration of GABA in GAD65-positive puncta or in insulin granules (Fig. 2f–h). Furthermore, we could not identify any marker for synaptic vesicles or endosomes that strongly colocalized with GAD65 vesicles or GABA in human or rat beta cells (SV2C, synapsin 6, synaptophysin, syntaxin, VAMP2, VGAT, WIPI2, APPL1, caveolin, clathrin, EEA1, GOPC, LAMP1, LC3, Rab3c, Rab5, Rab6, Rab7, Rab8, Rab9, Rab10 and Rab11 were tested). Yet, synaptic vesicle markers show strong colocalization with both GAD65 and GABA in neurons (Fig. 2h,i and Extended Data Fig. 2). Together, these results indicate that the magnitude of GABA release from beta cells does not involve synaptic-like microvesicles.

Islet GABA secretion is pulsatile, and depends on GABA content. To investigate GABA secretion from islets we used cellular biosensors[43–45] (Fig. 3 and Extended Data Fig. 3). GABA secretion in real time was monitored by recording intracellular Ca^{2+} mobilization ($\Delta[Ca^{2+}]_i$) in biosensor cells stably expressing heteromeric $GABA_B$ receptors ($GABA_B$ R1b and $GABA_B$ R2) and the G-protein α subunit, Gαqo5 (refs. [46,47]) (Extended Data Fig. 3). We found that GABA is secreted from human islets in rhythmic bursts (Fig. 3a) independent of glucose concentration. Biosensor responses could be blocked by the selective $GABA_B$ receptor antagonist CGP55845 (10 µM) (Fig. 3b) and did not occur in the absence of islets (Fig. 3a), confirming that the $[Ca^{2+}]_i$ responses were elicited by GABA released from islet cells. Pulsatile GABA secretion had distinct periods that in most islet preparations ranged from 4 to 10 min (Fig. 3c), similar to pulsatile insulin secretion in humans[48]. The periodicity of GABA secretion varied little between islets from the same human islet preparation. Calibrating biosensor responses from islets by comparing them with responses evoked by direct application of GABA in the same experiment, GABA release from a single islet was estimated to reach local concentrations above 10 µM. In conclusion, GABA secretion from islets is robust and pulsatile.

We performed experiments addressing the possibility of conventional Ca^{2+}-dependent exocytosis by granules or vesicles[31]. Stimulating islets with glucose had no effect on pulsatile GABA secretion measured by biosensor cells (Fig. 3d,e) or on total GABA secretion measured by HPLC (Fig. 3f and Extended Data Fig. 4) (see also refs. [33,34]). Depolarizing islets with KCl (30 mM) or removing extracellular Ca^{2+} did not affect pulsatile GABA secretion (Fig. 3g–i). Likewise, depleting extracellular calcium or simultaneously depleting intracellular Ca^{2+} sources with thapsigargin (Fig. 3j), stimulating with KCl (Extended Data Fig. 4) or opening ATP-gated potassium channels with diazoxide (Extended Data Fig. 4) did not significantly affect GABA secretion from human islets as measured by HPLC. Together, these results strongly suggest that Ca^{2+} (either influx or intracellular release) is not a primary trigger for gating of GABA release from the human islet.

A nonvesicular mode of GABA efflux likely depends on the cytosolic, metabolic pool of GABA[49,50]. Inhibiting GABA biosynthesis with allylglycine (10 mM) acutely diminished beta-cell GABA content and secretion (Fig. 3k,m and Extended Data Fig. 5). Increasing the intracellular GABA concentration by inhibiting GABA catabolism with γ-vinyl GABA (10 µM) increased the amount of released GABA per pulse (Fig. 3l,m). Thus, the effects of manipulating GABA metabolism are surprisingly acute and suggest a high rate of GABA biosynthesis that couples GABA efflux to the cytosolic GABA pool[34,51–53].

VRAC and TauT transport cytosolic GABA across the plasma membrane in islet cells. In view of the high levels of nonvesicular GABA release from beta cells, we sought to determine whether membrane transporters contribute to GABA efflux. We analyzed three distinct human islet single-cell RNA sequencing (RNA-seq) datasets[54–56] for expression of GABA-transporting proteins. A phylogenic tree of the neurotransmitter transporter family shows the relationship among the membrane GABA transporters (GAT1-3), the betaine-GABA transporter (BGT1) and TauT (Fig. 4a). GAT1-3 and BGT1 were not detected in beta cells (Fig. 4b and Extended Data Fig. 6). However, TauT, which is also a GABA transporter[57,58], is highly expressed in beta cells (Fig. 4b and Extended Data Fig. 6). Immunostaining confirmed expression and localization of TauT in the plasma membrane of human beta cells (Fig. 4c).

We further searched for other putative GABA transporters across the entire solute channel (SLC) gene group (395 members). Relative messenger RNA expression of all SLC genes in beta cells (Supplementary Table 2) revealed that the 4F2 cell-surface antigen heavy chain (4F2HC) and its heterodimer partners, LAT1 and LAT2, are highly expressed in beta cells (Fig. 4b and Supplementary Table 2). We considered LAT2 as a possible GABA transporter due to its specificity for the GABA-mimetic drug gabapentin[59]. Immunostaining confirmed islet-specific expression and localization

Fig. 2 | Subcellular localization suggests a nonvesicular GABA release mechanism in beta cells. a, A human islet from a nondiabetic donor immunostained for VGAT, insulin and somatostatin. Image is representative of the dataset plotted in panel **b**. Scale bar, 50 µm. Right panels show higher magnification views. Scale bar, 10 µm. **b**, Expression of VGAT is strongest in human delta cells and rat alpha cells but rare in beta cells of either species. Human islets stained for VGAT and insulin ($n=8$ islets, 3 donors), glucagon ($n=7$ islets, 3 donors) and somatostatin ($n=5$ islets, 3 donors). Rat islets stained for VGAT and insulin ($n=7$ islets, 3 donors), glucagon ($n=6$ islets, 3 donors) and somatostatin ($n=6$ islets, 3 donors). One-way ANOVA: insulin versus somatostatin, human (*$P<0.0001$); insulin versus glucagon, rat (*$P<0.0001$). Center line indicates the mean. **c**, GABA is nonvesicular and cytosolic in almost all human beta cells. A $VGAT^{NEG}$ primary human beta cell immunostained for GABA, VGAT and insulin (not shown). Image is representative of $n=3$ human islet preparations, ≥3 samples per preparation. Scale bar, 50 µm. Right panels show higher magnification views. Scale bar, 2 µm. **d**, A rare $VGAT^{POS}$ primary human beta cell showing colocalization of GABA and VGAT in vesicular structures. Image is representative of $n=3$ human islet preparations, ≥3 samples per preparation. Scale bar, 50 µm. Bottom panels show higher magnification views. Scale bar, 2 µm. **e**, A primary human delta cell immunostained for GABA, VGAT and somatostatin (not shown) showing colocalization of GABA and VGAT in vesicular structures. Image is representative of $n=3$ human islet preparations, ≥3 samples per preparation. Scale bar, 50 µm. Bottom panels show higher magnification views. Scale bar, 2 µm. **f**,**g**, GABA is present in the cytosol and does not colocalize with insulin or GAD65 in vesicular structures in primary human (**f**) or rat (**g**) beta cells immunostained for GABA, insulin and GAD65. Images are representative of $n=3$ islet preparations, ≥3 samples per preparation. Scale bar, 10 µm. Inset images show single-channel higher magnification views. Scale bar, 2 µm. **h**, Colocalization between GAD65 (green) and synaptic vesicle markers synaptophysin, SV2C and VGAT (red) or GABA (red) in primary human beta cells, primary rat beta cells and primary rat hippocampal neurons. Images are representative of data plotted in **i**. Scale bar, 2 µm. **i**, Quantification of colocalization in human beta cells for GAD65 with markers of synaptic vesicles synaptophysin ($n=14$), SV2C ($n=3$) and VGAT ($n=10$); in primary rat beta cells ($n=11$, 10 and 10); and primary rat hippocampal neurons ($n=6$, 11 and 11). While GAD65-positive vesicles in rat neurons colocalize with synaptic vesicle markers, colocalization is rare or absent in human and rat beta cells. Two-way ANOVA: human beta cells versus rat neurons for all markers (*$P<0.0001$), rat beta cells versus rat neurons for all markers (*$P<0.0001$).

of both 4F2HC and LAT2 in the plasma membrane of human islet cells (Fig. 4d).

Uptake of ^{3}H-radiolabeled GABA (^{3}H-GABA) was measured to assess whether either TauT or LAT2 mediates inward transport of GABA in human islets (Fig. 4e). Competing substrates for TauT (10 mM taurine, beta-alanine) or LAT2 (10 mM leucine) were tested for inhibition of ^{3}H-GABA uptake. Unlabeled GABA served as a positive control and glycine served as an additional control for possible GABA transport by monoamine transporters. Taurine and beta-alanine strongly inhibited uptake of ^{3}H-GABA similarly to unlabeled GABA, while leucine and glycine were less effective (Fig. 4e). Pharmacological inhibition of the membrane GABA transport family with a mixture of SNAP5114 (50 µM), NNC05-2090 (50 µM) and NNC711 (10 µM) also inhibited ^{3}H-GABA uptake. These GAT inhibitors also perturbed pulsatile GABA release measured by biosensor cells (Extended Data Fig. 4), producing an initial transient increase in extracellular GABA levels, indicating that GABA uptake is important for maintaining low interstitial

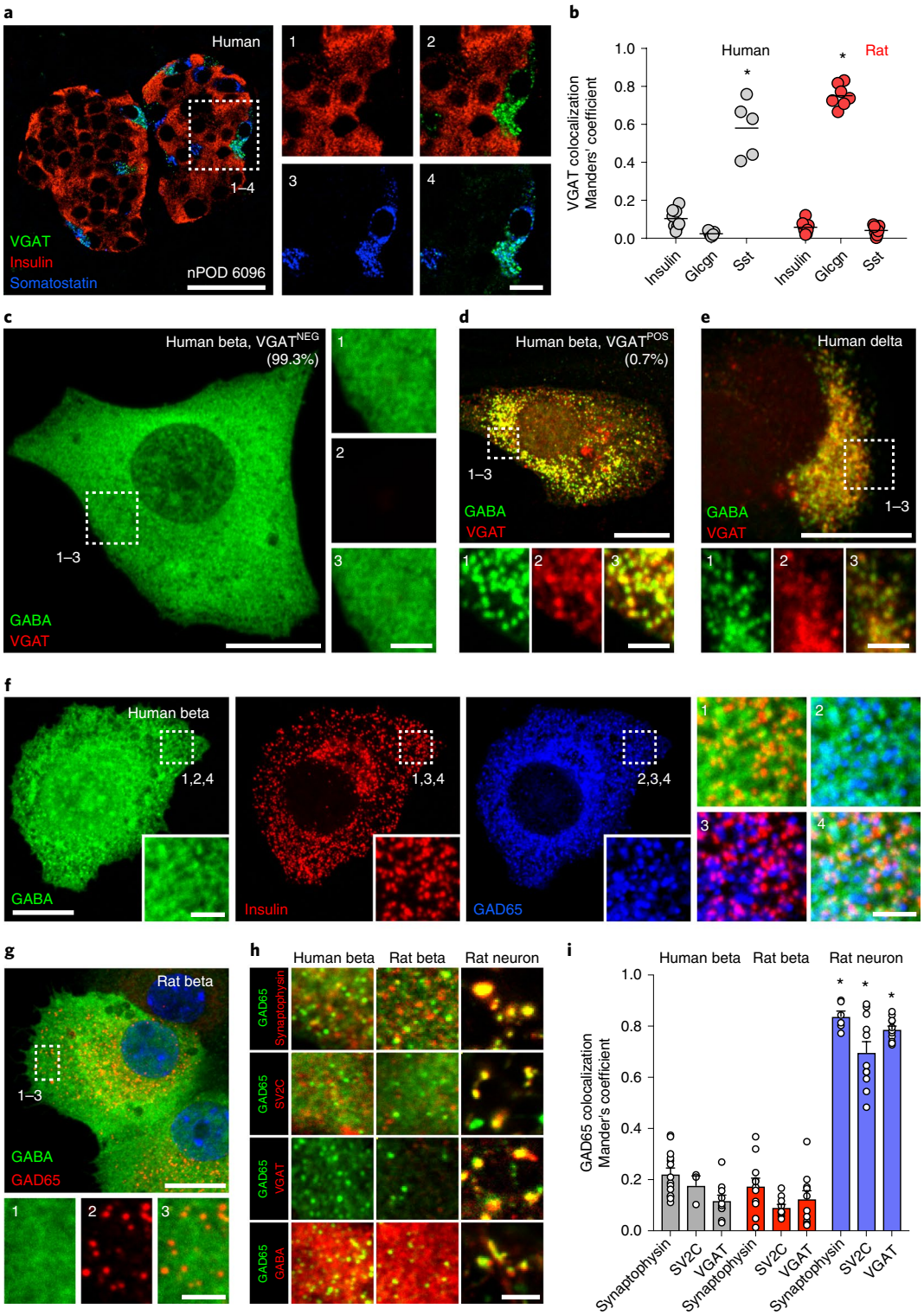

levels in the islet. As we were unable to detect expression of GAT1-3 in islet cells, we propose that the GAT-blocking drugs acted on closely related TauT. Together, the data support the conclusion that TauT is the dominant mediator of GABA uptake in islets.

For GABA release, we looked for expression of known noncanonical GABA transporters, including bestrophin chloride channels (BEST1-4)[60] and VRAC[61]. VRAC conveys osmo-sensitive chloride (Cl^-) currents and conducts efflux of GABA, taurine and other small organic osmolytes to regulate cell volume[61–64]. VRAC complexes are heterohexamers composed of multiple LRRC8 family subunits, LRRC8A, B, C, D or E. LRRC8A (also known as Swell1) is critical for formation of functional VRAC channels while its heteromer partners LRRC8B-E confer substrate specificity[61,65]. VRAC subunit LRRC8D confers permeability to GABA and taurine[62]. Beta cells express VRAC[66–68], with channel subunits LRRC8A, LRRC8B and LRRC8D detected by single-cell RNA-seq (Fig. 4b).

To assess whether VRAC channels mediate GABA efflux, human islets were exposed to hypo-osmotic buffer and release of endogenous GABA was measured by HPLC (Fig. 4f). GABA release increased by threefold or 40-fold on exposure to increasingly hypotonic buffer (Fig. 4f). Hypotonic induction of GABA efflux was eliminated from LRRC8A knockout MIN6 beta cells[67] and isotonic GABA efflux was reduced by ~50% (Fig. 4g,h). These results support a mechanism of cytosolic GABA release from islets via VRAC.

To assess whether VRAC in beta cells is responsible for generation of GABA release pulses, we generated beta-cell-specific LRRC8A knockout mice (βc-*LRRC8A*$^{-/-}$) by crossing *LRRC8A* floxed mice (*LRRC8A*$^{fl/fl}$)[67,69] with mice expressing Cre recombinase in insulin-producing beta cells (*Ins1*^{cre})[70]. Loss of LRRC8A in islets isolated from βc-*LRRC8A*$^{-/-}$ mice was confirmed by western blot (Fig. 4i). βc-*LRRC8A*$^{-/-}$ islets do not release GABA in response to hypotonic stimulus (Fig. 4j), consistent with beta cells being the dominant GABA-synthesizing cell type in the islet. In wild-type *LRRC8A*$^{+/-}$ littermates, GABA release was pulsatile in isotonic conditions and responded to continuous hypotonic stimulation with kinetics consistent with VRAC gating[62]: delayed activation of GABA release of 2–3 min that builds to a maximum rate of release after ~8 min and remains active throughout the hypotonic stimulation. Biosensor cell recording of GABA release from βc-*LRRC8A*$^{-/-}$ islets demonstrated both a loss of GABA pulses and loss of GABA release under hypotonic stimulus (Fig. 4k,l and Extended Data Fig. 7). We next studied the effect of knocking down LRRC8A in human islets transduced with adenovirus encoding LRRC8A short hairpin RNA (shRNA) (Ad-mCherry-hLRRC8A-shRNA) or scrambled shRNA (Ad-mCherry-scramble-shRNA) (Fig. 4l–n). Expression of adenovirus LRRC8A shRNA resulted in ~40% decrease in expression of LRRC8A and loss of GABA pulses (Fig. 4m–o). Finally, we used HPLC, a direct detection method, to validate that the kinetics of GABA released from human islets under hypotonic stimulation are consistent with previous reports of VRAC-mediated organic osmolyte release (Fig. 4p)[62]. Together, these data are consistent with a critical role of the LRRC8A component of VRAC in release of GABA from the cytosol of beta cells.

Cytosolic GABA secretion synchronizes insulin secretion. GABA has been assigned many functional and regulatory roles in the islet. However, its effects on hormone secretion in human beta cells has been a matter of ongoing investigation[71]. We examined the autocrine effects of pulsatile GABA release on insulin secretion from human islets. Exposure of human islets at 5 mM glucose to exogenous GABA (10 μM) reduced insulin release by ~40%, suggesting that GABA has an inhibitory effect on insulin release under normoglycemic conditions (Fig. 5a). We next measured the effect of decreasing endogenous GABA release by inhibiting GABA biosynthesis with allylglycine (10 mM) (Fig. 5b). Inhibition of endogenous islet GABA production increased insulin secretion during glucose stimulation (11 mM) (Fig. 5b,c), consistent with an inhibitory effect of GABA on insulin secretion. Inhibition of endogenous islet GABA production did not, however, affect insulin release stimulated by depolarization with KCl (Fig. 5b), indicating that allylglycine treatment did not disrupt the available pool of releasable insulin.

We next measured the effect of GABA on cytosolic Ca^{2+} responses in human islets. Human islets were loaded with Ca^{2+} indicator dye (Fluo4) and imaged by confocal microscopy during glucose stimulation (Fig. 5d,e). When GABA was applied during the first phase of glucose-induced Ca^{2+} influx, cytosolic Ca^{2+} levels were quickly and dramatically reduced to near prestimulation levels. Islets quickly desensitized within 1–2 min to the inhibitory effect of applied GABA. These effects are consistent with GABA acting through $GABA_A$ ionotropic receptors (rather

Fig. 3 | Islet GABA secretion is pulsatile and depends on GABA content. a, GABA release from a human islet maintained in 3 mM glucose, detected by cytosolic Ca^{2+} flux in $GABA_B$ receptor-expressing biosensor cells (black trace). Biosensor cell responses to no islets or to GABA only are shown for comparison (blue traces). Unless otherwise specified, in this and Figs. 4–6, the plot shows the average 340/380 Fura-2 ratio from ≥5 GABA biosensor cells located under the islet, hereafter labeled as GABA release. This is a representative trace of experiments performed on $n = 40$ human islet preparations. **b**, The $GABA_B$ receptor antagonist CGP55845 (10 μM) blocks biosensor cell detection of GABA pulses from a single human islet. Results are representative of $n = 3$ human islet preparations, ≥3 islets per preparation. **c**, Periods of pulsatile GABA release measured from $n = 22$ human islet preparations, ≥3 islets per preparation. Mean ± s.e.m. **d**, Representative trace of GABA release pulses from a human islet at different glucose concentrations (1G = 1 mM, 3G = 3 mM, 11G = 11 mM). Results are representative of data plotted in panel **e**. **e**, Quantification of traces shows no difference in the amount of released GABA per pulse at different glucose concentrations ($n = 3$ islet preparations, 18–20 islets per preparation). One-way ANOVA: 1G versus 3G (NS, $P = 0.6181$), 1G versus 11G (NS, $P = 0.1684$), 3G versus 11G (NS, $P = 0.5302$). Mean ± s.e.m. **f**, Insulin and GABA released during human islet perifusion. GABA and insulin were quantified in the same sample by HPLC and ELISA ($n = 3$ samples of 100 islets each). One-way ANOVA: for insulin release, 3G versus 16.7G (*$P = 0.0046$), 3G versus KCl (*$P = 0.0007$); for GABA release, 3G versus 16.7G (NS, $P = 0.5034$), 3G versus KCl (NS, $P = 0.2341$). **g**, Islet GABA secretory pulses before and during (shaded area) KCl depolarization (30 mM). Trace is representative of $n = 3$ human islet preparations, ≥3 islets per preparation. **h**, Islet GABA secretory pulses in the presence and absence (shaded area) of nominal Ca^{2+}. Trace is representative of $n = 3$ human islet preparations, ≥3 islets per preparation. **i**, Quantification of GABA release during KCl depolarization and absence of nominal Ca^{2+} compared with control ($n = 15$ islets, 3 donors). Two tailed *t*-test: KCl versus hypothetical mean of 1.0 (*$P = 0.0069$), 0 Ca^{2+} versus hypothetical mean of 1.0 (NS, $P = 0.1202$). Mean ± s.e.m. **j**, HPLC quantification of GABA release from human islets in the presence and absence of nominal Ca^{2+}, with or without thapsigargin (10 μM) inhibition of intracellular Ca^{2+} ($n = 4$ samples of 100 islets each). One-way ANOVA: control versus 0 Ca^{2+} (NS, $P = 0.5231$), control versus 0 Ca^{2+} + thapsigargin (NS, $P = 0.2946$), 0 Ca^{2+} versus 0 Ca^{2+} + thapsigargin (NS, $P = 0.8851$). Mean ± s.e.m. **k**, Trace of GABA release from a human islet before (black trace) and after (red trace) applying the GAD65 inhibitor allylglycine (10 mM). Trace is representative of $n = 3$ islet preparations, ≥3 islets per preparation. **l**, Trace of GABA release from a human islet before (black trace) and after (green trace) applying the GABA transaminase inhibitor γ-vinyl GABA (10 μM). Trace is representative of $n = 3$ islet preparations, ≥3 islets per preparation. **m**, Quantification of GABA release from human islets treated with allylglycine or γ-vinyl GABA ($n = 3$ islet preparations, ≥4 islets per preparation). Two-tailed student's *t*-test: control versus allylglycine (*$P = 0.0353$), control versus γ-vinyl GABA (*$P = 0.0411$). Mean ± s.e.m. AUC, area under the curve.

than $GABA_B$ metabotropic receptors)[72]. GABA applied to islets in resting glucose conditions (3 mM) had no effect on beta-cell Ca^{2+} calcium responses.

To test the effects of GABA on coordinated pulsatile insulin secretion, we measured serotonin release as a surrogate for insulin secretion[73–77] using Chinese hamster ovary (CHO) cells expressing the serotonin receptor 5-HT2C (refs. [78,79]). As we and others have reported[77,79–81], serotonin/insulin secretion from human islets was pulsatile with regular periods ranging from 4 to 10 min (Fig. 5f). When we decreased endogenous GABA levels and release from cells by inhibiting GABA biosynthesis with allylglycine (10 mM), basal serotonin/insulin secretion increased and failed to display regular secretory pulses (Fig. 5f,h). Decreasing catabolism of GABA and increasing endogenous GABA levels by adding γ-vinyl-GABA (10 μM) inhibited pulsatile serotonin/insulin secretion (Fig. 5g,h). Similarly, blocking $GABA_A$ receptor signaling with the inhibitor SR 95531 (10 μM) disrupted the periodicity of serotonin pulses (Fig. 5i). These results indicate that GABA production and paracrine GABAergic signaling within the islet impact periodic insulin secretion.

By expressing the lumenal protein of large dense core vesicles, neuropeptide Y (NPY), fused to the pH-dependent green fluorescent protein pHluorin in beta cells, we visualized exocytotic events in real time[82,83] and observed periodic exocytotic bursts occurring simultaneously throughout the islet with periods of ~5 min. In the presence of the $GABA_A$ receptor agonist muscimol (100 μM) these exocytotic events became smaller and lost synchronicity (Fig. 5j,k).

Thus, using four different methods, we provide evidence that endogenously produced GABA released from a cytosolic beta-cell pool decreases insulin release while stabilizing the periodicity and glucose responsiveness of insulin secretion.

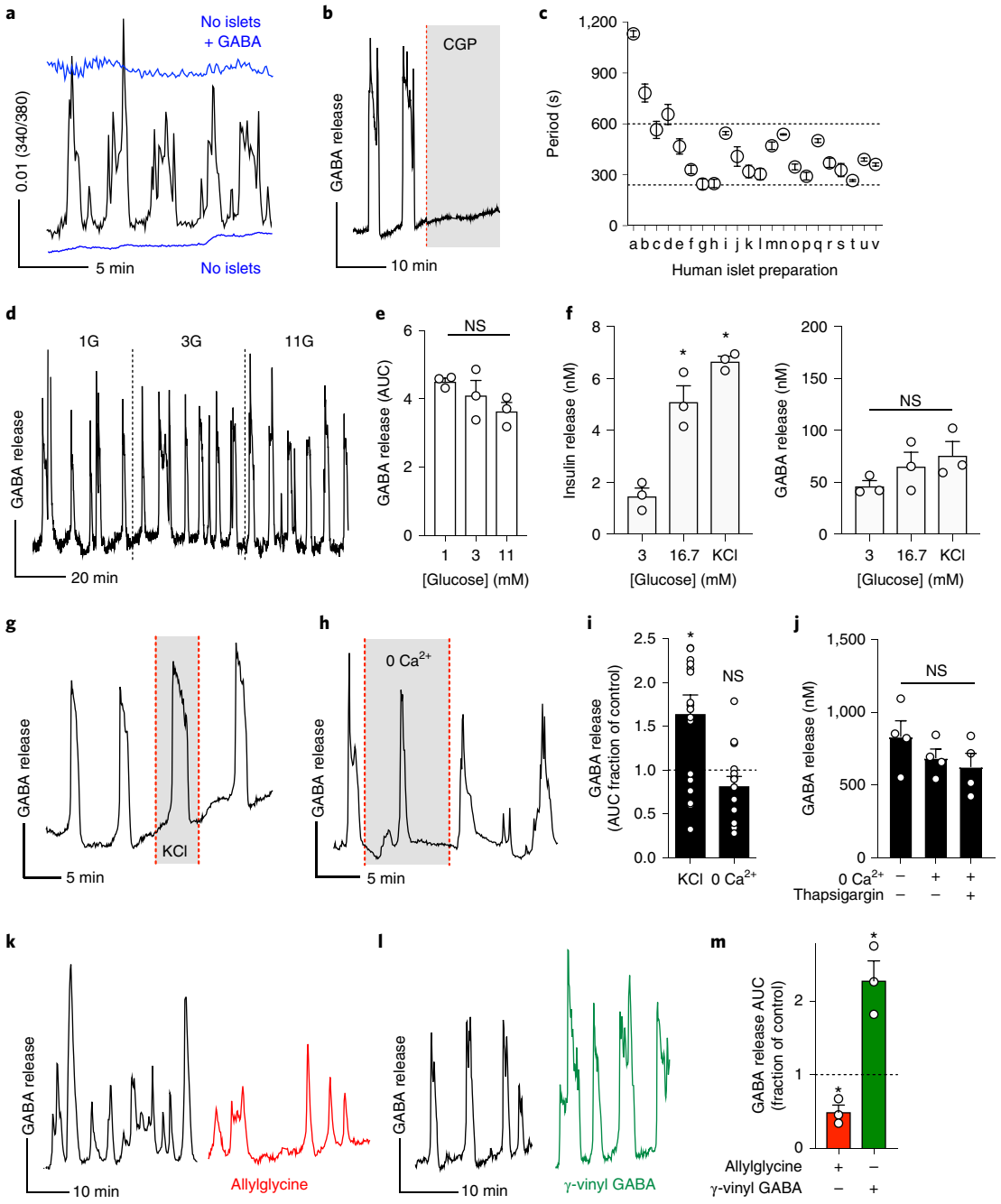

Cytosolic GABA secretion is interrupted in human islets from type 2 diabetic donors. As shown in Fig. 1, immunostaining of human islets from type 2 diabetic donors revealed depletion of GABA pools in beta cells in spite of robust expression of the biosynthesizing enzyme GAD65. We examined multiple preparations from human type 2 diabetic donors for GABA release with biosensor cells ($n \geq 3$ islets from each of the five donors). Consistent with the immunostaining results, we could not detect pulsatile GABA secretion from human islets from type 2 diabetic donors (Fig. 6a,b). Type 2 diabetic islets did respond to KCl depolarization as evidenced by a strong increase in cytosolic Ca^{2+}, indicating that they were alive and retained membrane potentials (Fig. 6c). By contrast, pulsatile GABA secretion was robust in islets from nondiabetic donors (Fig. 6a, see also Fig. 3). Pulsatile GABA secretion from islets of patients with type 2 diabetes could be rescued by inhibiting GABA catabolism with γ-vinyl GABA (10 μM) (Fig. 6d,e). The periodicity of insulin release, measured by serotonin co-release detected via biosensor cells, was deranged in type 2 diabetic islets (Fig. 6f,g). This effect was similar to that elicited by blocking GABA signaling in nondiabetic islets by inhibiting $GABA_A$ receptors with SR 95531 (Fig. 5i). Insulin secretion periodicity in type 2 diabetic islets became more regular on treatment with γ-vinyl GABA (Fig. 6g).

We previously reported the accumulation of GAD65 in Golgi membranes of beta cells undergoing ER stress through perturbations of the palmitoylation cycle that controls targeting of the enzyme to peripheral vesicles[84]. Similar accumulation and defect in membrane compartment distribution were detected in individuals experiencing early as well as late phases of GAD65 autoimmunity and development of type 1 diabetes[84]. We examined the intracellular distribution of GAD65 by confocal microscopy of immunostained sections of human pancreas. GAD65 was detected in both the cytoplasm and Golgi compartment in beta cells in sections from nondiabetic donors (Fig. 6h), but showed increased localization to the Golgi compartment in beta cells of patients with type 2 diabetes (Fig. 6i,j).

Discussion

Our study provides evidence for a mechanism of GABA release in human beta cells. As a result of enzymatic synthesis of GABA from glutamic acid by GAD65, GABA is present at high levels in the cytoplasm of beta cells. It is from this cytosolic pool that GABA is released, because only ~1% of the beta cells show evidence of VGAT expression and the consequent accumulation of GABA in secretory vesicles. Our study shows that GABA in the islet behaves as an organic osmolyte. Indeed, in the islet, GABA shares transport properties with the canonical organic osmolyte taurine, namely efflux via VRAC and uptake via TauT. We further found that islet GABA levels are greatly reduced under diabetic conditions. Given the paracrine, islet-trophic and immunosuppressive roles of GABA, the loss of islet GABA content in both type 1 and type 2 diabetes may contribute to beta-cell loss and dysfunction.

Several mechanisms can be suggested to cause the low levels of islet GABA in human diabetes. First, while the GAD67 isoform binds the co-enzyme 5′-pyridoxal phosphate firmly and is a constitutively active holoenzyme, GAD65 oscillates between an active holoenzyme and an inactive apo-enzyme[85,86]. Thus, it is possible that GAD65 is mainly present as an inactive apo-enzyme in beta cells under diabetic conditions. Second, GAD65 may be rendered

Fig. 4 | VRAC and TauT transport cytosolic GABA across the plasma membrane in beta cells. a, Phylogenetic tree diagram of human SLC6A neurotransmitter transporter family members. **b**, Gene expression for SLC6A and other proteins of interest for GABA transport and biosynthesis in human beta cells from an analysis of a curated human islet single-cell RNA-seq dataset ($n = 158$ cells)[56]. Mean ± s.e.m. Results are representative of three different human single-cell RNA-seq datasets analyzed (Extended Data Fig. 6 and Supplementary Table 1). **c**, Representative confocal image of a human pancreas section immunostained for TauT and insulin. Scale bar, 50 μm. Right panels show higher magnification views of the boxed region with individual channels for TauT (1) and insulin (2). Image is representative of $n = 3$ donors, ≥3 islets per donor. Scale bar, 20 μm. **d**, Representative confocal microscopy images of an islet in a human pancreas section immunostained for LAT2 (upper panel) and 4F2HC (lower panel). Scale bar, 50 μm. Right panels show higher magnification views of the boxed region showing individual channels for LAT2 (1) and 4F2HC (2). Image is representative of $n = 3$ donors, ≥3 islets per donor. Scale bar, 20 μm. **e**, Uptake of radiolabeled ^{3}H-GABA by human islets with competitive inhibition from unlabeled GABA, taurine, beta-alanine, leucine or glycine; or blocking the GABA transporters with a mixture of SNAP5114 (50 μM), NNC05-2090 (50 μM) and NNC711 (10 μM) (GAT blockers) ($n = 3$ samples of 500 islets each). One-way ANOVA: control versus GABA ($^*P < 0.0001$), control versus taurine ($^*P < 0.0001$), control versus β-alanine ($^*P < 0.0001$), control versus glycine ($^*P < 0.0001$), control versus GAT blockers ($^*P < 0.0001$), control versus leucine ($^{\#}P = 0.0139$). Data are representative of three islet preparations (two human, one rat). Center line indicates the mean. **f**, HPLC measurement of cumulative GABA and taurine release from human islets in KRBH buffer of varying osmolarity ($n = 3$ samples, 100 islets each). One-way ANOVA: for GABA, 300 versus 160 mOsm l^{-1} ($^*P < 0.0001$), 300 versus 250 mOsm l^{-1} ($^*P = 0.0288$). Data are representative of four human islet preparations. Center line indicates the mean. **g**, Western blot for LRRC8A and β-actin in wild-type (WT) and *LRRC8A*$^{-/-}$ MIN6 insulinoma cells. Results are representative of three independent immunoblots with similar results. **h**, HPLC measurements of rate of GABA release from WT or *LRRC8A*$^{-/-}$ MIN6 insulinoma cells during static incubation in 3 mM glucose isotonic (300 mOsm l^{-1}) or hypotonic (250 mOsm l^{-1}) KRBH buffer ($n = 3$ samples of 40,000 cells each). WT and *LRRC8A*$^{-/-}$ MIN6 cells were transfected with a plasmid encoding human GAD65 24 h before the experiment as they do not endogenously express either GAD65 or GAD67. Two-way ANOVA: WT iso versus WT hypo ($^*P < 0.0001$), WT iso versus *LRRC8A*$^{-/-}$ iso ($^*P = 0.0053$), *LRRC8A*$^{-/-}$ iso versus *LRRC8A*$^{-/-}$ hypo (NS, $P = 0.2974$). Center line indicates the mean. **i**, Western blot for LRRC8A in mouse islets isolated from WT (*LRRC8A*$^{+/-}$ littermates heterozygous for floxed allele) and beta-cell-specific knockout (βc-*LRRC8A*$^{-/-}$) mice. Western blot was performed once using islets pooled from two donors of each genotype. **j**, HPLC measurements of cumulative GABA release from WT and βc-*LRRC8A*$^{-/-}$ mouse islets in 3 mM glucose isotonic (300 mOsm l^{-1}) or hypotonic (250 mOsm l^{-1}) KRBH buffer. $n = 3$ samples of 20 islets each. Two-way ANOVA: WT iso versus WT hypo ($^*P < 0.0001$), βc-*LRRC8A*$^{-/-}$ iso versus βc-*LRRC8A*$^{-/-}$ hypo (NS, $P = 0.8057$). Mean ± s.e.m. **k**, Biosensor cell traces of GABA release from WT and βc-*LRRC8A*$^{-/-}$ mouse islets during isotonic and prolonged (10 min+) hypotonic stimulation. Islets used for these experiments were confirmed for loss of LRRC8A by western blot (panel **g**). Results are representative of data plotted in panel **l**. **l**, GABA release detected by biosensor cells from WT ($n = 5$) and βc-*LRRC8A*$^{-/-}$ ($n = 3$) mouse islets. Data are representative of two independent islet isolations. Two-way ANOVA of log-transformed data: WT iso versus WT hypo ($^*P = 0.0003$), WT iso versus βc-*LRRC8A*$^{-/-}$ iso ($^*P = 0.0003$), βc-*LRRC8A*$^{-/-}$ iso versus βc-*LRRC8A*$^{-/-}$ hypo (NS, $P = 0.9999$). Mean ± s.e.m. **m**, Western blot for LRRC8A in human islets infected with Ad-mCherry-scramble-shRNA or Ad-mCherry-hLRRC8A-shRNA adenovirus. Western blot was performed once. **n**, Knockdown of LRRC8A in human islets reduces basal GABA pulses. Results are representative of the data plotted in panel **o**. **o**, Quantification of biosensor cell detection of GABA release from human islets infected with Ad-mCherry-scramble-shRNA ($n = 3$ islets) or Ad-mCherry-hLRRC8A-shRNA ($n = 6$ islets). Data are representative of two independent human islet preparations. Two-tailed *t*-test ($^*P = 0.0065$). Mean ± s.e.m. **p**, HPLC measurement of dynamic GABA release from nondiabetic human islets during isotonic (300 mOsm l^{-1}) and prolonged hypotonic (250 mOsm l^{-1}) stimulation. $n = 3$ samples of 100 islets each. Mean ± s.e.m. CPM, counts per minute; iso, isotonic; hyper, hypertonic; hypo, hypotonic; scr, scramble.

inactive in beta cells by expression or formation of an inhibitor. Third, GABA metabolism, rather than GAD65 expression, may be a dominant factor controlling islet GABA content in beta cells in diabetic conditions.

GAD65 anchors to the cytosolic face of intracellular membranes[25]. The shift in localization of the enzyme to perinuclear ER/Golgi membranes observed in beta cells in human diabetes would not be expected to prevent release of the product GABA into the cytosol unless the enzyme in Golgi membranes represents the inactive GAD65 apo-enzyme or is associated with an inhibitor. The consequent decrease in synthesis of cytosolic GABA would interrupt GABA transport and prevent pulsatile GABA secretion. This possibility would be consistent with our observations in human alpha cells, which are devoid of GABA, yet express GAD65 that appears to localize exclusively to ER/Golgi membranes.

Expression of the synaptic vesicle markers VGAT and synaptophysin in islets[87,88] has contributed to the concept that GABA is secreted from beta cells via synaptic-like microvesicles[28]. Here, using an approach that allows for high-resolution subcellular localization studies, we show that almost all beta cells (>99%) lack synaptic-like vesicles or granules containing VGAT together with GAD65 and/or GABA. A small subset of beta cells (<1%) exhibit all features of vesicular GABA. The nature of the small subpopulation of VGAT-positive beta cells is currently unknown but may intersect with

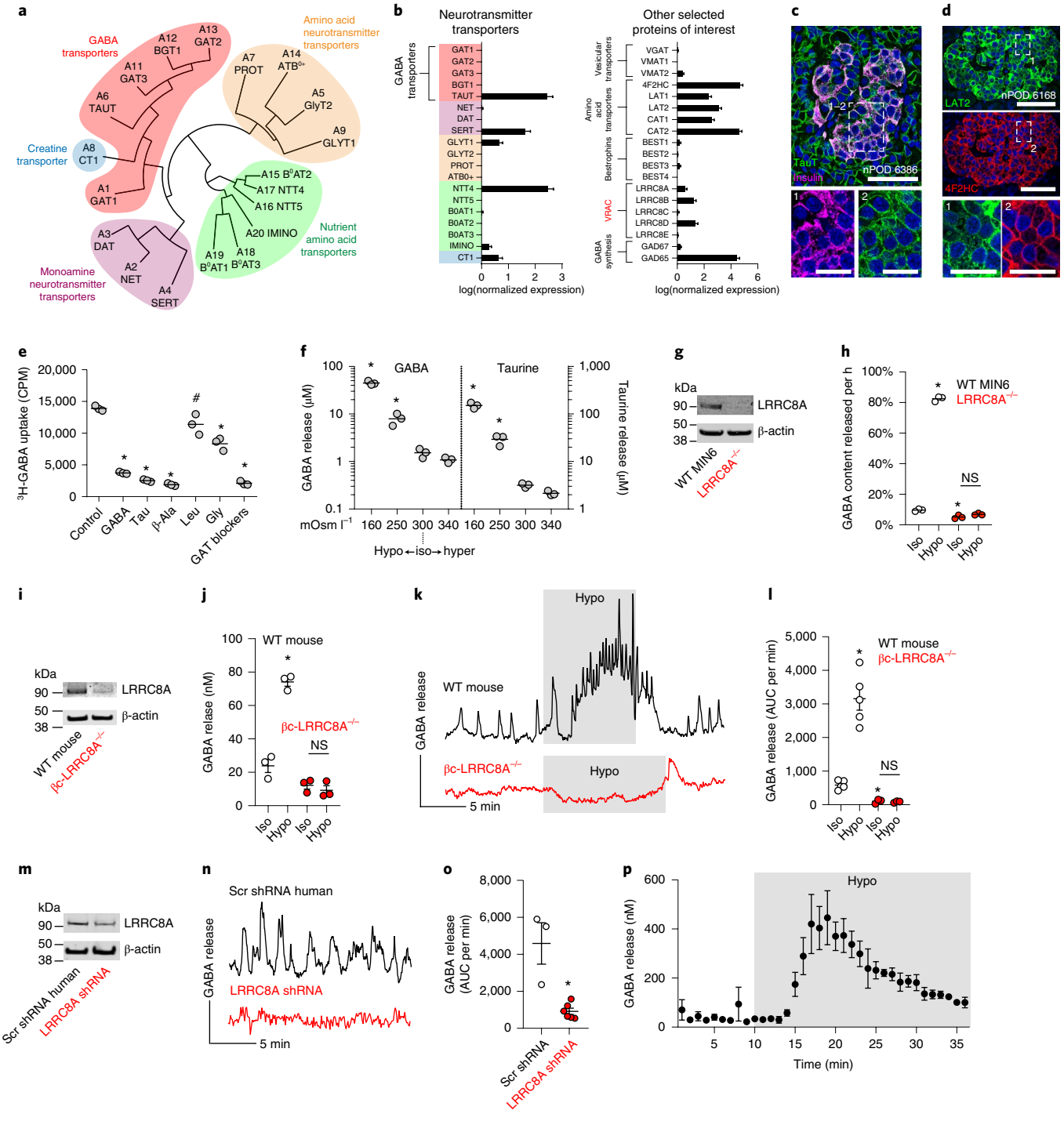

markers of beta-cell subtype and/or maturation state. It is possible that its size is variable and subject to presently unknown factors, which could affect its contribution to the vesicular release of GABA described earlier[26,31,89]. However, it appears that in the vast majority of beta cells, GABA is released from the cytosolic pool via plasma membrane channels.

Pertinent to our findings, Rorsman and Pipeleers have previously reported a high rate of basal (nonquantal) GABA release that was unregulated by glucose or pharmacological regulators of insulin secretion[31,34,90]. Due to this unregulated GABA release, it was concluded that the beta cell must be equipped with a second pathway for release of GABA that is nonvesicular, the details of which remained to be elucidated[31,90]. Here, we have identified VRAC to be a pathway for GABA release.

While glucose-inducible VRAC Cl^- currents have been observed in beta cells[67,68], no effect of glucose has been reported for LRRC8A-dependent organic osmolyte efflux. This may be because LRRC8A-dependent Cl^- and organic osmolyte efflux are not required to follow the same behavior. For example, organic osmolyte and Cl^- currents can occur through different isoforms of the VRAC channel. LRRC8A/D is the dominant channel for GABA release and LRRC8A/B/C/E channels exhibit low GABA conductance but high Cl^- conductance[62,65]. It remains to be determined whether multiple isoforms of VRAC exist simultaneously in beta cells or whether the same VRAC channel can differentially gate Cl^- and organic osmolytes depending on the activating conditions. Another explanation for why we do not observe glucose-mediated effects on GABA release may be that the degree of swelling required to activate the GABA VRAC channel is greater than obtained by glucose stimulation. The Jentsch group reported that a very high, nonphysiological glucose stimulation (25 mM) induced comparatively moderate beta-cell swelling (only 1/4 of the volume differential of hypotonic stimulation) and no clear subsequent regulatory volume decrease[68]. The Sah group obtained similar results, where they showed that 16.7 mM glucose induces only a minor beta-cell swelling of 6.8% in murine beta cells with a sluggish associated volume response, and no clear trend of glucose on human beta-cell swelling[67]. If regulatory volume decrease is required for organic osmolyte efflux via VRAC, then this lack of a regulatory volume decrease on glucose stimulation is consistent with our observation that glucose does not induce GABA release.

Our findings indicate that endogenously released GABA has two major effects on beta cells: (1) it reduces insulin secretion and (2) it helps stabilize the periodicity of insulin pulses. That GABA has inhibitory effects on beta cells was further supported by experiments in which GABA and the $GABA_A$ receptor agonist muscimol were added exogenously, and is consistent with findings by Birnir and colleagues[71]. Similar to the role somatostatin is proposed to play in the islet[91,92], GABA may serve to change the gain of insulin secretion and thus prevent its wasteful release. The pulsatile pattern of GABA efflux and its impact on the periodicity of insulin secretion suggest an additional role for GABA in timing or pacing of oscillatory islet activities. As shown by our results, restoring GABA signaling in type 2 diabetic islets improves the synchronicity of insulin secretory pulses but diminishes their magnitude. Conversely, the loss of GABA in diabetic states is likely to produce increases in the excitability of beta cells that will help increase insulin secretion, but at the price of losing periodicity. While continuous pulsatile GABA release may contribute to the economy and periodicity of insulin secretion under normal conditions, it remains to be determined whether the dramatic reduction in GABA levels is a mechanism that helps the beta cell increase insulin secretion and hence cope with the increased demand in diabetic states.

Our findings that GABA inhibits insulin secretion and beta-cell Ca^{2+} responses differ from those showing that GABA depolarizes beta cells and increases insulin secretion[31]. The discrepancy can be explained by different experimental conditions (for example, dynamic hormone secretion measurements versus static incubation, different basal glucose concentrations). That GABA has been reported to depolarize beta cells to approximately −50 mV (ref. [31]), however, indicates that GABA will clamp the membrane potential below the threshold for the opening of P/Q-type Ca^{2+} channels (above −20 mV), the channels that are responsible for insulin granule exocytosis[93]. Our findings are further in line with results showing that GABA stimulates delta cells[31], which leads to secretion of the potent inhibitory hormone somatostatin. Importantly, beta cells also express inhibitory metabotropic $GABA_B$ receptors whose activation opens hyperpolarizing K^+ channels or inhibits adenylyl cyclases[94]. Therefore, there is substantial evidence supporting an inhibitory role for GABA in human beta cells.

It is likely that many physiological processes within the islet, including local actions of secreted GABA and of other paracrine signals[31,43,44], shape islet cell excitability, as described for neurons in the central nervous system[36,95]. In addition to the effects on insulin secretion reported here, nonvesicular GABA secretion also affects the activities of the glucagon-secreting alpha cell and the somatostatin-secreting delta cell[27,96]. Because GABA stimulates delta cells to secrete somatostatin and because somatostatin strongly inhibits insulin secretion, a pulse of GABA may inhibit beta cells

Fig. 5 | Cytosolic GABA secretion synchronizes insulin secretion. a, Human islet perifusion in 5 mM glucose showing reversible inhibition of insulin secretion in response to exogenous GABA (10 μM). $n = 3$ islet preparations. Mean ± s.e.m. **b**, Human islet perifusion showing differential glucose-stimulated insulin response in islets treated with GAD65 inhibitor allylglycine (10 mM, red trace) versus control (black trace). $n = 3$ islet preparations. Mean ± s.e.m. **c**, Quantification from islet perifusion during 11 mM glucose stimulation phase, control (black trace), with allylglycine (red trace). $n = 3$ islet preparations (average of >3 islets per preparation). Two-tailed *t*-test, $^*P = 0.0175$. Mean ± s.e.m. **d**, Four independent traces of cytosolic Ca^{2+} levels measured by Fluo-4 dye in human islets during successive addition of 3 mM glucose, 16.7 mM glucose and GABA (10 μM). GABA induces a rapid drop in cytosolic Ca^{2+} that desensitizes after ~90 s. Data are representative of three human islet preparations. **e**, Quantification of ΔCa^{2+} levels in human islets under 16.7 mM glucose stimulation during the first 2 min after addition of GABA. $n = 4$ islets. Two-tailed *t*-test, $^*P = 0.0132$. Mean ± s.e.m. **f**, Effect of the GAD65 inhibitor allylglycine (10 mM) on serotonin/insulin secretion from human islets at 3 mM glucose concentration using serotonin biosensor cells. Trace is representative of experiments performed in $n = 3$ human islet preparations, ≥3 islets per preparation. **g**, Effect of the GABA transaminase blocker γ-vinyl GABA (10 μM) on serotonin/insulin secretion from human islets at 3 mM glucose concentration. Ca^{2+} trace is representative of experiments performed in $n = 3$ human islet preparations, ≥3 islets per preparation. **h**, Quantification of serotonin/insulin secretion from human islets treated with allylglycine or γ-vinyl GABA from experiments performed. $n = 3$ human islet preparations, ≥3 islets per preparation. One-way ANOVA, $^*P < 0.0001$. Mean ± s.e.m. **i**, Periodicity of serotonin/insulin secretion from human islets ($n = 28$ biosensor cells) and the increase in periodicity variance in the presence of the $GABA_A$ receptor antagonist SR 95531 (10 μM) ($n = 35$ biosensor cells). Data are pooled from three independent human islet preparations, >3 islets per preparation. Two-sided *F*-test to compare variances, $^*P = 0.0002$. Mean ± s.e.m. **j**, Traces of the sum of fluorescent exocytotic signals in three individual beta cells from different islet regions showing periodic, synchronous exocytosis at 16 mM glucose (left) and asynchronous, diminished exocytosis after adding the $GABA_A$ receptor agonist muscimol (100 μM, right). Traces are representative of $n = 3$ islet preparations, ≥3 islets per preparation. **k**, Quantification of the amplitude of beta-cell fluorescent exocytotic signals in islets treated with muscimol. $n = 3$ human islet preparations, ≥3 islets per preparation, all measurements depicted. Two-tailed *t*-test, $^*P < 0.0001$. Mean ± s.e.m. 5HT, serotonin.

both directly and indirectly via delta cells. Recent findings by the Sah and Jentsch groups demonstrate that knockout of LRRC8A, the GABA-releasing pathway we report here, impairs glucose-responsive insulin secretion, in contrast to our finding that GABA is inhibitory to beta cells[67,68]. A possible explanation for this discrepancy is that insulin secretion is an event requiring integration of multiple signals. Sah and Jentsch both showed that loss of LRRC8A also affects beta-cell membrane potential and delays or impairs beta-cell Ca^{2+} responses. As GABA appears to only be inhibitory to beta cells during glucose-responsive Ca^{2+} fluxes, any loss of inhibition from impaired GABA release may be overwhelmed by the stronger inhibition imposed by LRRC8A knockout. Thus, the functional effect of a loss of GABA is observable by blocking GABA biosynthesis, as we have shown, but not by preventing GABA release through VRAC knockout.

Intracellular GABA levels and cytosolic GABA release are dramatically decreased in type 1 (Fig. 1) and type 2 diabetes (Figs. 1 and 6), indicating that islets lose the paracrine, trophic and immunomodulatory influence of GABA in the diabetic state. It is conceivable that this loss of GABA leaves islets vulnerable to destructive inflammation. We propose that a periodic pattern of cytosolic GABA release independent of glucose concentration impacts the magnitude and periodicity of insulin secretion. Interrupting GABA secretion impairs coordination of hormone secretion. Irregular

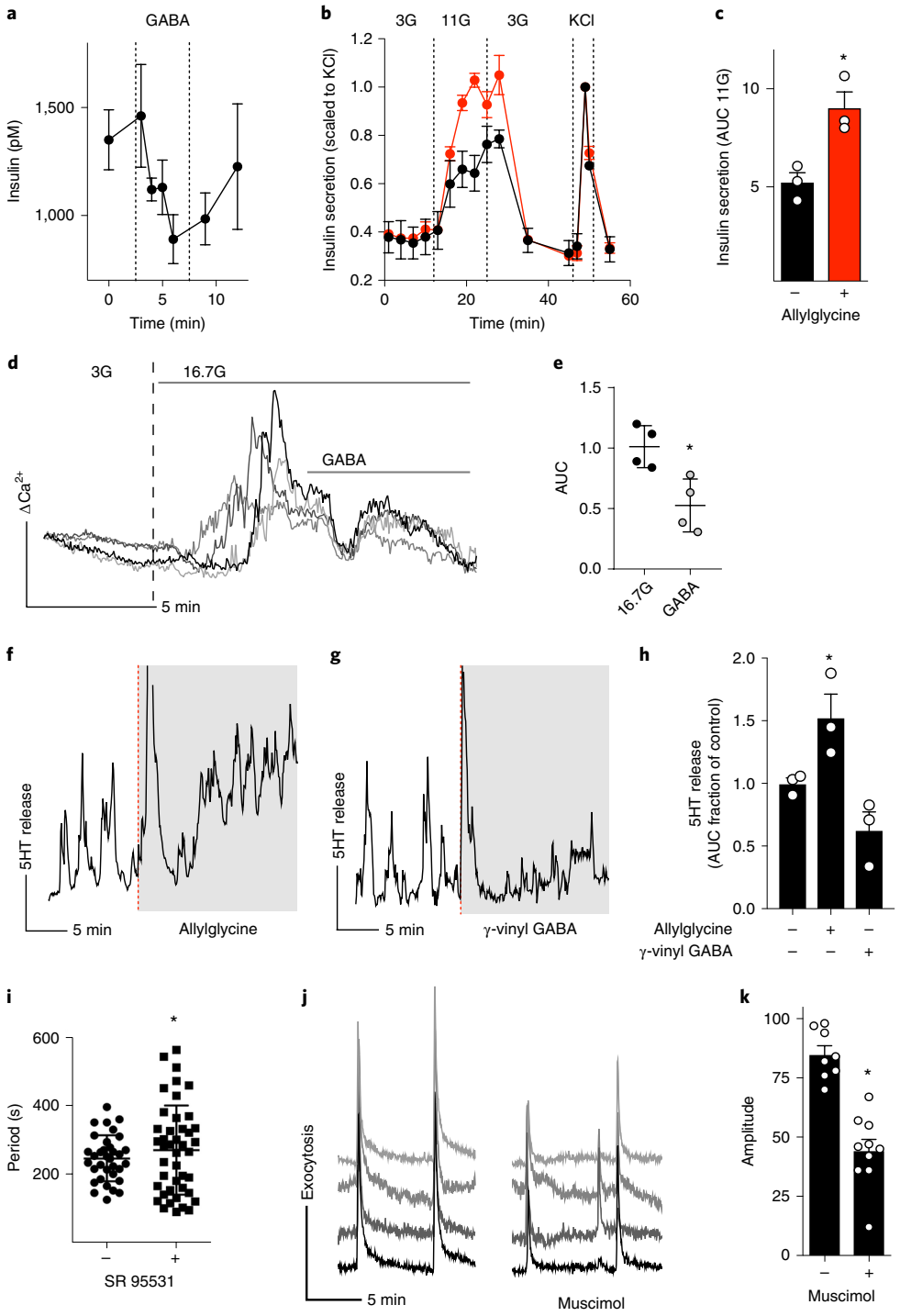

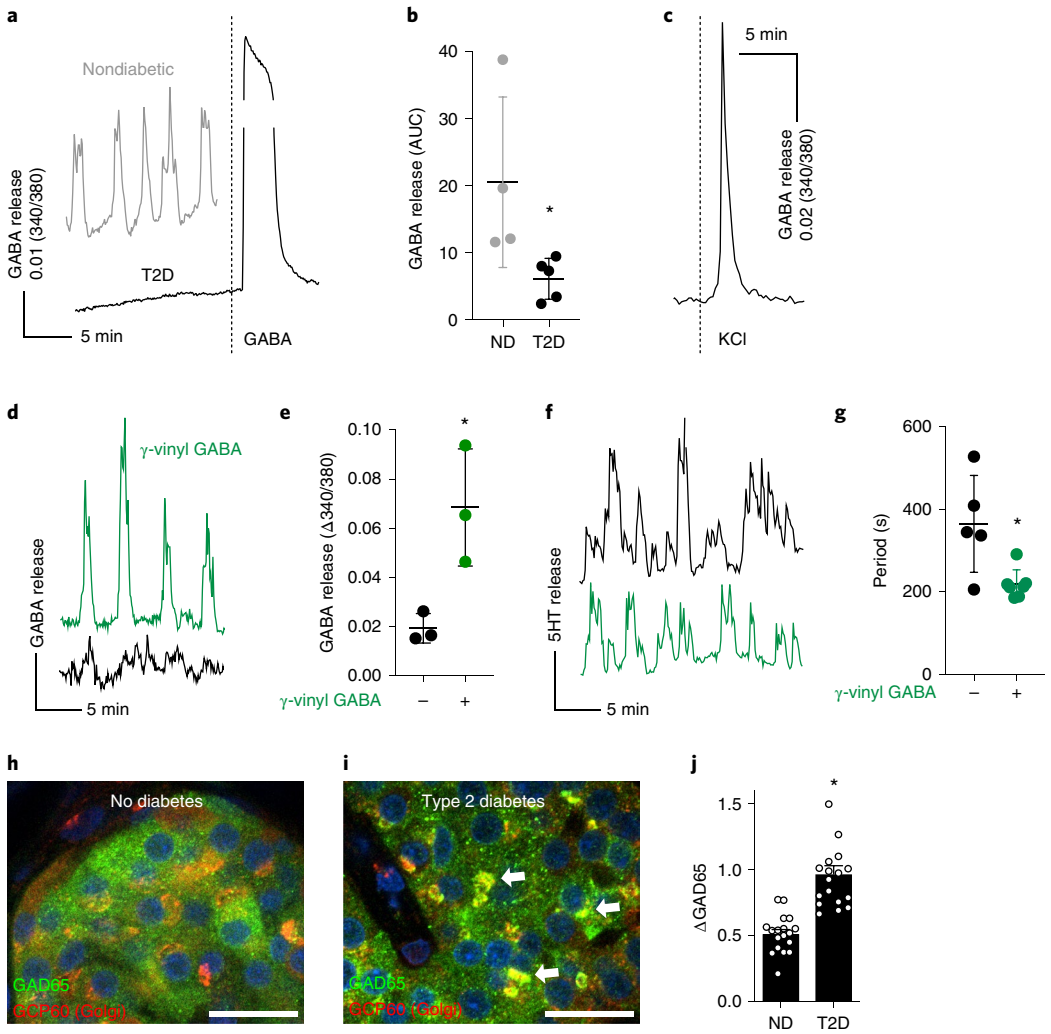

Fig. 6 | Cytosolic GABA secretion is interrupted in human islets from type 2 diabetic donors. a, Absence of GABA secretion detected by biosensor cells from an islet taken from a type 2 diabetic donor (black trace), but distinct GABA secretion is detected from an islet from a nondiabetic donor (gray trace). Addition of exogenous GABA to a type 2 diabetic islet induces a strong response from biosensor cells. Representative of experiments performed in five islet preparations from type 2 diabetic donors and 40 nondiabetic donor preparations, ≥3 islets per preparation. **b**, Quantification of GABA release from nondiabetic ($n=4$) and type 2 diabetic ($n=5$) human islets. Two-tailed t-test, $^*P=0.0418$. Mean ± s.e.m. **c**, Ca^{2+} flux in diabetic human islets during stimulation with KCl. Representative of experiments performed in five islet preparations from diabetic donors. **d**, Pulsatile GABA release from an islet from a type 2 diabetic donor before (black trace) and after (green trace) exposure to the GABA transaminase inhibitor γ-vinyl GABA (10 µM, 1 h). Representative of $n=5$ islets. **e**, Quantification of GABA release pulse amplitude from type 2 diabetic human islets before and after exposure to γ-vinyl GABA. $n=3$ human islet preparations (average of ≥3 islets per preparation). Two-tailed t-test, $^*P=0.0257$. Mean ± s.e.m. **f**, Insulin/serotonin release detected by serotonin biosensor cells from an islet from a type 2 diabetic donor before (black trace) and after (green trace) exposure to γ-vinyl GABA (10 µM, 1 h). Representative of $n=5$ islets. **g**, Periods of insulin/serotonin release from islets from a type 2 diabetic donor before (black dots) and after (green dots) exposure to γ-vinyl GABA (10 µM, 1 h) from experiments performed as in **f**. $n=5$ islets. Two-tailed t-test to compare means, $^*P=0.01$; two-sided F-test to compare variances, $^*P=0.0118$. Mean ± s.e.m. **h**,**i**, Confocal images of islets from nondiabetic (**h**) and type 2 diabetic donors (**i**) immunostained for GAD65 and Golgi resident protein GCP60. Arrows point at GAD65 accumulation in Golgi membranes. Images are representative of data plotted in panel **j**. Scale bar, 10 µm. **j**, Quantification of GAD65 immunostaining intensities in Golgi membranes in beta cells of pancreata from nondiabetic and type 2 diabetic donors. GAD65 staining in Golgi membranes is expressed relative to the total cellular GAD65 staining (ΔGAD65). $n=18$ islets from three donors per group. Two-tailed t-test, $^*P<0.0001$. Mean ± s.e.m..

insulin secretion from the islet may exacerbate insulin resistance[48]. Given its inhibitory effect on alpha cells, defective GABA signaling[97] and decreased GABA secretion could also explain why glucagon secretion is increased in type 2 diabetes, causing further elevation of hyperglycemia. Thus, loss of GABA signaling in the islet may contribute to the pathogeneses of type 1 and 2 diabetes. Because restoring GABA signaling can be proposed as an intervention point to promote islet function, our study has implications for a pharmaceutical strategy for the treatment of diabetes. In rodent islets, electrical coupling via gap junctions and purinergic paracrine signaling have been suggested to coordinate rhythmic insulin secretion[48]. Here, we show, however, that in the human islet GABA is a potential pacemaker candidate, because (1) it is released independently of glucose concentration in pulses with a frequency in the range of those of pulsatile in vivo insulin secretion, (2) it is a diffusible factor acting on $GABA_A$ receptors whose activation inhibits beta-cell activity and (3) its production and release can regulate the periodicity of insulin secretion.

Methods

Human pancreas tissues. Human pancreatic sections from tissue donors of both sexes were obtained via the Network for Pancreatic Organ Donors with Diabetes (nPOD) tissue bank, University of Florida. Human pancreata were harvested from cadaveric organ donors by certified organ procurement organizations partnering with nPOD in accordance with organ donation laws and regulations and classified as 'Non-Human Subjects' by the University of Florida Institutional Review Board (IRB) (IRB no. 392-2008), waiving the need for consent[98,99]. nPOD tissues specifically used for this project were approved as nonhuman by the University of Florida IRB (IRB no. 201701113).

Human pancreatic islets were obtained from deceased nondiabetic donors and from donors with type 2 diabetes from the Human Islet Cell Processing Facility at the Diabetes Research Institute at the University of Miami Miller School of Medicine, from the National Institute of Diabetes and Digestive and Kidney Diseases-funded Integrated Islet Distribution Program at City of Hope, from the European Consortium on Islet Transplantation Islets for Basic Research Program and from Prodo Laboratories. Human pancreatic islets from deceased donors with type 1 diabetes were isolated by the nPOD Islet Isolation Program. Human islets received from the University Hospital of Geneva and San Raffaele Scientific Institute, Milan, through the European Consortium on Islet Transplantation Islets for Basic Research Program were approved by the IRB of the University Hospital of Geneva and Commission Cantonale d'Ethique de la Recherche (CCER no. 05-028) and by the Ethics Committee of the San Raffaele Scientific Institute of Milan (IPF002-2014). The University of Geneva and the San Raffaele Institute Ethics Committees waived the need for consent from the donors because islets were used for experimental research only when not suitable for clinical purposes and would otherwise have been destined for destruction. In such cases, obtaining informed consent is not mandatory in Switzerland and Italy. Cadaveric human islets for research were approved as nonhuman by the University of Florida IRB (IRB no. 201702860).

Human islets were cultured at 24 °C in 10-cm nonadherent cell culture dishes (500 islets per dish) in CMRL medium with 2% glutamine, 10% fetal bovine serum (FBS), 10 mM HEPES and 1% penicillin/streptomycin.

Rat pancreatic islets. All experimental protocols using rat islets were approved by the University of Florida and École Polytechnique Fédérale de Lausanne (EPFL) Animal Care and Use Committees. Rat islets were isolated from pancreases of male and female postnatal day 5 (P5) Sprague Dawley rats (Charles River) in accordance with published methods[1]. Rat pups were killed by decapitation and the whole pancreas was removed and digested in 0.15 mg ml^{-1} Liberase TL (Roche no. 05401020001) in Hank's buffered salt solution (HBSS) (Gibco no. 24020091) with 20 mM HEPES for 7 min with strong manual agitation. The Liberase enzyme was stopped with addition of HBSS, 20 mM HEPES and 0.5% FBS. Digested pancreas tissue was washed four times with HBSS, 20 mM HEPES and 0.5% FBS at 4 °C, resuspended in Histopaque-1119 (Sigma no. 11191), overlain with HBSS, 20 mM HEPES and 0.5% FBS (room temperature), and centrifuged for 20 min at 300*g* at 20 °C. Islets were collected from the interface between Histopaque and HBSS phases and washed three times with HBSS, 20 mM HEPES and 0.5% Newborn calf serum (NBCS). Islets were then hand-cleaned with a 200-µl pipette and cultured in 10-cm nonadherence petri dishes at 37 °C and 5% CO_2, with 500 islets per dish, and 9 ml RPMI 1640 medium with GlutaMAX (Gibco no. 61870010), 10% FBS and 1% penicillin/streptomycin.

LRRC8A knockout mouse islets. All experimental protocols using transgenic mice were approved by the University of Florida Animal Care and Use Committee. Experimental protocols using transgenic mouse islets were approved by the University of Florida Animal Care and Use Committee. *LRRC8A*-floxed (*LRRC8A*$^{fl/fl}$) mice on the C57BL/6NCrl background were generated in and provided by Rajan Sah's laboratories at the University of Iowa and Washington University in St. Louis[67,69]. *LRRC8A*$^{fl/fl}$ mice were crossed with mice expressing Cre recombinase in beta cells (Ins1^{cre})[70] purchased from The Jackson Laboratory (B6(Cg)-*Ins1*$^{tm1.1(cre)Thor}$/J; stock no. 026801) to generate beta-cell-specific LRRC8A knockout (βc-*LRRC8A*$^{-/-}$) mice. Mouse genotypes were confirmed by PCR using published primers[67,69,70] and loss of LRRC8A in islets was confirmed by western blot. βc-*LRRC8A*$^{-/-}$ mice (8–14 weeks old) were killed by cervical dislocation under deep isoflurane anesthesia according to the approved procedures. Heterozygous *LRRC8A*$^{+/-}$ Cre-expressing littermates served as wild-type controls. Equal numbers of male and female mice were used. The pancreas was perfused via the common bile duct with 2–3 ml HBSS containing Liberase TL (0.15 mg ml^{-1}), removed and digested at 37 °C for an initial 12 min, disrupted by pipetting up and down several times with a 10-ml pipette and digested for a final 4 min. The enzyme digestion was quenched with HBSS and 10% FBS. Islets were purified from digested tissue and cultured using the same methods as described for rat islets.

Islet cell monolayer culture. Within 1 week of isolation, rat or human islets were hand-picked from suspension cultures, collected in a 15-ml tube and washed twice in PBS without Ca^{2+} and Mg^{2+}. Islets were dissociated into a suspension of single islet cells by continuous gentle pipetting in 0.3 ml 0.05% trypsin-EDTA per 500 islets for 3 min at 37 °C. Trypsin digestion was halted by addition of islet monolayer medium (minimum essential medium (MEM) with GlutaMAX 11 mM glucose, 5% FBS, 1 mM sodium pyruvate, 10 mM HEPES and 1× B-27 Supplement) to a total volume of 15 ml, followed by pelleting of islet cells by centrifugation for 5 min at 1,400 r.p.m. (350*g*) and resuspension islet monolayer medium. Islet cells were seeded on round 12-mm diameter and 0.17-mm thickness borosilicate glass coverslips (Electron Microscopy Sciences) coated with purified laminin (Gibco) or purified collagen IV (Sigma Aldrich) at 50 µg ml^{-1} in HBSS with Ca^{2+}/Mg^{2+} for 1 h at 37 °C. Cells were seeded at approximately 35,000 cells per cm^2. Islet cells required 3–4 d of culture to adhere and spread on surfaces before further experimentation. A detailed description and validation of monolayer cultures of primary human and rat islets cells is available[100].

Hippocampal neuron cultures. Primary rat hippocampal neurons were prepared from P2–P3 Sprague Dawley rats of both sexes, as described by Codazzi et al.[101]. Neurons were seeded on round poly-L-ornithine-coated glass or Thermanox coverslips (Nunc), at 100,000 cells per coverslip in a 24-well plate and in 1 ml neuronal medium: MEM with GlutaMAX (Gibco), 11 mM glucose, 5% FBS, 1 mM sodium pyruvate, 10 mM HEPES and 1× B-27 Supplement (Gibco). At 1 d after isolation, 3 µM of the chemotherapeutic agent ARA-C (Sigma-Aldrich) was added to the culture medium to eliminate astrocytes and obtain a neuronal culture of high purity (>90% neurons).

Immunofluorescence staining. Human pancreas sections obtained from nPOD were deparaffinized followed by acidic-pH heat-mediated antigen retrieval according to the nPOD standard operating procedure for immunopathology. Monolayers of pancreatic islet cells were fixed with 4% EM-grade PFA (Electron Microscopy Sciences) at room temperature for 20 min. Samples were blocked and permeabilized in PBS with 0.3% Triton X-100 with 10% goat or donkey serum. Primary antibodies were incubated overnight in PBS with 0.3% Triton X-100 with 1% goat or donkey serum at 4 °C. Alexa Fluor 405-, 488-, 568- and 647-conjugated secondary antibodies (Thermo Fisher) were incubated at 1:200 dilution in PBS with 0.3% Triton X-100 for 30 min at room temperature. Coverslips were mounted with ProLong Gold Antifade Reagent with or without DAPI (Thermo Fisher).

Immunostaining for GABA and taurine was validated by competitive inhibition of primary antibody binding by addition of soluble GABA or taurine to the antibody incubation buffer (Extended Data Fig. 6). The anti-GABA and anti-taurine antibodies showed minimal nonspecific binding toward non-GABA or nontaurine amino acids. Furthermore, GABA immunostaining was eliminated by inhibition of the GABA-synthesizing enzyme, GAD65, with allylglycine (Extended Data Fig. 5).

Microscopy. Confocal images (pinhole = 1 airy unit) of randomly selected islets (2–3 islets per section) were acquired on a confocal laser-scanning microscope (Zeiss LSM700, Zeiss LSM710, Leica SP5 and Leica SP8) with ×20/0.8 numerical aperture Plan-Apochromat air-, and ×40/1.30 and ×63/1.40 numerical aperture Plan-Apochromat oil-immersion objectives at 1,024 × 1,024 pixel resolution. Images were processed and quantified in ImageJ. Manders' coefficient colocalization analyses were performed using the JACoP (Just Another Colocalization Plugin) plugin for ImageJ[102]. To determine the subcellular localization of GAD65, the intensity of GAD65 immunostaining in the Golgi compartment of beta cells in pancreata from healthy donors was compared with that of pancreata from type 2 diabetes donors. Using ImageJ software, we measured GAD65 staining intensity in the whole cells as well as in the Golgi apparatus by selecting a region of interest based on the Golgi staining signal. GAD65 immunostaining was always more intense in the Golgi apparatus than in the cytosol. To allow comparisons between tissue sections and specimens, we expressed the mean GAD65 staining intensity in the Golgi compartment relative to the intensity of GAD65 staining in the whole beta cell (ΔGAD65 = (mean GAD65 intensity in Golgi − mean GAD65 intensity in whole cell)/mean GAD65 intensity in whole cell).

Gene expression analysis. Raw molecular counts per gene and cell were directly obtained from the Gene Expression Omnibus (accession numbers GSE84133, GSE81076 and GSE83139), and further normalized using the R package scran[103]. Results were qualitatively similar across the three datasets. log(norm_values + 1) corresponding to GSE81076 are displayed in Fig. 4 and corresponding to GSE84133 and GSE83139 in Extended Data Fig. 6.

Detection of GABA via biosensor cells. We adapted real-time measurements of GABA secretion from Dvoryanchikov et al.[104]. GABA biosensor cells were obtained from Novartis Institutes for BioMedical Research in Switzerland. GABA biosensor cells consisted of CHO cells stably expressing heteromeric $GABA_B$ ($GABA_B$ R1b and $GABA_B$ R2) receptors and the G-protein α subunit, Gαqo5, modified to couple to increases in $[Ca^{2+}]_i$ via the $InsP_3$ signaling cascade (Extended Data Figs. 3 and 7). GABA biosensor cells reliably responded to low concentrations of GABA (threshold ≈ 100 nM), making them highly sensitive GABA detectors. GABA biosensor cell responses were measured using $[Ca^{2+}]_i$ imaging. We loaded GABA biosensors with the $[Ca^{2+}]_i$ indicator Fura-2 and plated them on poly-D-lysine-coated cover slips in a perfusion chamber. Individual human islets were

placed on top of this layer of biosensor cells. Fluid perfusion was performed with a gravity-driven Warner Instruments VC-8 eight-channel perfusion system set to 0.5–1 ml min^{-1} and connected to a Warner Instruments RC-20 closed bath small-volume imaging chamber to ensure linear solution flow and fast exchange. GABA secretion was examined in biosensor cells located immediately downstream of the islet in recordings lasting at least 20 min to be able to detect rhythmic behavior. GABA secretion was examined for pulses simply by inspecting recordings for robust increases in $[Ca^{2+}]_i$ in biosensor cells. Because the pulse amplitudes were large, no deconvolution or other processing of the raw $[Ca^{2+}]_i$ traces was necessary. We calculated the periods between pulses by measuring the time between the initial rises in $[Ca^{2+}]_i$ in at least three sequential pulses per biosensor cell. The regularity of the pulses was quantified by using the deviation of this interpulse interval. Changes in the amount of secreted GABA were quantified by measuring the area under the curve of the $[Ca^{2+}]_i$ responses in the biosensor cells during defined time intervals. These analyses were only performed within the same experiment because quantitative comparisons between experiments would have required calibration with known concentrations of GABA. Only recordings with at least three responsive biosensor cells were included in the analyses. Secretion was considered coordinated and pulsatile if the responses in the biosensor cells were synchronized and showed regular periods. We expressed these data as average traces of the $[Ca^{2+}]_i$ responses of the biosensor cells.

We established that biosensor cells responded only to GABA and not to other substances including taurine. Of all the tested substances, only GABA activated the biosensor. Crucially, the antagonist CGP (10 µM) completely blocked $GABA_B$ receptors on the GABA biosensors and eliminated responses generated from islets. Stimuli or pharmacological agents (for example, antagonists, transporter blockers) used in this study did not themselves either elicit biosensor responses or alter the ability of biosensors to respond to GABA. We conducted these controls by $[Ca^{2+}]_i$ imaging of biosensor cells plated at low density and in the absence of islets. When examining pulsatile secretion, it was important to establish that biosensor cells themselves did not display periodic behavior in the absence of islets or in the continuous presence of GABA. Biosensor cells for acetylcholine, which are also CHO cells, did not show oscillatory responses in the presence of islets[44], indicating that oscillatory signals are not an intrinsic property of these cells but stem from the islet's secretory behavior. The effects of manipulation were compared with controls recorded in the same experimental session or using islets from the same human islet preparation to compensate for the variability in the quality of islets. To ensure that islets were healthy, we simultaneously monitored $[Ca^{2+}]_i$ responses in islets and biosensor cells. KCl depolarization induced responses in islets but not in biosensor cells, indicating that islet cells were viable. False negative results were ruled out by confirming that biosensor cells remained fully responsive to GABA at the end of the recording session.

Detection of insulin via biosensor cells. To detect insulin release we used an approach in which serotonin is used as a surrogate for insulin. Serotonin is present in insulin granules and is released with insulin[73–77,81]. Biosensor cells for serotonin were CHO cells expressing the serotonin receptor $5\text{-}HT_{2C}$ and are further described and characterized in previous publications[78,79].

Determination of cytosolic Ca^{2+} concentration. Imaging of cytoplasmic $[Ca^{2+}]$ ($[Ca^{2+}]_i$) was performed in accordance with published descriptions[105]. Islets, dispersed islet cells or biosensor cells were incubated in Fura-2 acetoxymethyl ester, (2 µM; 1 h) and placed in a closed small-volume imaging chamber (Warner Instruments). Stimuli were applied with the bathing solution. Cells loaded with Fura-2 were alternatively excited at 340 and 380 nm light and fluorescence was recorded on two different microscope setups. At the University of Miami, we used a monochromator light source (Cairn Research Optoscan Monochromator, Cairn Research). Images were acquired with a Hamamatsu camera attached to a Zeiss Axiovert 200 microscope (Carl Zeiss). Changes in the 340/380 fluorescence emission ratio were analyzed over time in individual cells using MetaFluor imaging software. At the University of Florida, we used a pE-340fura light-emitting diode illumination system (CoolLED) and a Hamamatsu ORCA-Flash 4.0 LT+ camera attached to a Zeiss Axio Observer Z1 microscope. Changes in the 340/380 fluorescence emission ratio were analyzed over time in individual cells using Zeiss Zen 2.3 blue edition software.

Insulin secretion during perifusion. A high-capacity, automated perifusion system was used to dynamically measure insulin secretion from pancreatic islets (BioRep Perifusion V2.0.0). A low-pulsatility peristaltic pump pushed Kreb's ringer bicarbonate HEPES (KRBH) solution at a perifusion rate of 100 µl min^{-1} through a column containing 100 pancreatic islets immobilized in Bio-Gel P-4 Gel (BioRad). Except where otherwise stated, glucose concentration was adjusted to 3 mM for all experiments. Stimuli were applied with the perifusion buffer. The perifusate was collected in an automatic fraction collector designed for a 96-well plate format. The columns containing the islets and the perifusion solutions were kept at 37 °C, and the perifusate in the collecting plate was kept at <4 °C. Perifusates were collected every minute. Insulin release in the perifusate was determined with the human or mouse Mercodia Insulin enzyme-linked immunosorbent assay (ELISA) kit following the manufacturer's instructions.

KRBH buffer preparation. KRBH buffer (115 mM NaCl, 4.7 mM KCl, 2.5 mM $CaCl_2$, 1.2 mM KH_2PO_4, 1.2 mM $MgSO_4$, 25 mM $NaHCO_3$, 25 mM HEPES, 0.2% BSA, 3 mM glucose) was prepared containing final concentrations of solutes according to Supplementary Table 3. Theoretical osmolarity was calculated according to the following expression[106]:

$$\text{osmolarity} = \sum_i \varphi_i n_i C_i \quad (1)$$

where φ is the osmotic coefficient, n is the number of particles (for example, ions) into which a molecule dissociates, C is the molar concentration of the solute and i is the identity of a particular solute. Osmolarities of solutions were verified using an osmometer and found to be in good agreement with theoretical calculations. Isotonic KRBH had an osmolarity of 294 mOsm l^{-1}.

Detection of GABA by HPLC with electrochemical detector. Fractions collected from islet perifusion in the BioRep islet perifusion device or supernatants from static incubations in KRBH buffer were analyzed for GABA content using an EICOM HTEC-500 HPLC-ECD with autosampler, online automated *o*-phthalaldehyde-derivatization and Eicompak FA-3ODS separation column. This automated detection technique is linearly sensitive for GABA from the nano-molar to milli-molar range[107]. Insulin content in the same sample fraction was determined by ELISA kit (Mercodia). Data shown in Fig. 3f analyzed GABA content from perifusion fractions while data shown in Figs. 3j and 4f,h,j and Extended Data Fig. 4a–c are from static incubations. Each sample (for all cases) contained approximately 100 islet equivalents (IEQ). Perifusion flow rate was 100 µl min^{-1}. Static incubations were performed in 100 µl KRBH and 3 mM glucose for 30 min.

LRRC8A knockout MIN6 cells. Wild-type and *LRRC8A* (also known as *Swell1*) knockout MIN6 beta cells generated by CRISPR/Cas9 technology[67] were provided by Rajan Sah's laboratories at the University of Iowa and Washington University in St. Louis. Confirmation of *LRRC8A* gene disruption by PCR, *LRRC8A* protein deletion and ablation of LRRC8A-mediated current in these cells were published by the Sah group[67]. MIN6 cells cultured in DMEM with 15% FBS and 1% penicillin/streptomycin were transfected with human GAD65-GFP plasmid[39] using Lipofectamine 2000.

Adenovirus. Human adenovirus type 5 with hLRRC8A-shRNA (Ad5-mCherry-U6-hLRRC8A-shRNA) and with a scrambled nontargeting control (Ad5-U6-scramble-mCherry) was obtained from Vector Biolabs. Adenovirus was added to human islets in culture (final concentration of 5×10^7 plaque-forming units per ml) and incubated for 24 h. The islets were then washed with PBS three times and cultured for 1–2 d before performing further experiments. Transduction efficiency was assessed by fluorescence microscopy.

Western blotting. Cell lysates were prepared by extraction of whole islets or MIN6 cells in RIPA buffer (Sigma). The BCA protein assay kit (Thermo Fisher Scientific) was used to measure the protein concentration of cell extracts. Gel electrophoresis was performed with the NuPAGE system (Life Technologies) with transfer onto polyvinylidene fluoride membranes with the iBlot 2.0 (Life Technologies) device. Membranes were blocked with 5% nonfat milk in Tris-buffered saline, incubated in primary antibody overnight at 4 °C and detected with secondary antibody (LI-COR Biosciences). Blots were imaged on the LI-COR Odyssey CLx scanner.

Real-time recording of exocytosis. To image exocytosis, an adenovirus was engineered, encoding for an endogenous protein of large dense core vesicles, NPY, fused to pHluorin, a pH-dependent green fluorescent protein[108]. Human islets infected with this virus were cultured short term (1 week) to permit exogenous adenoviral protein expression while retaining islet cell function. The NPY-pHluorin fusion protein was correctly localized to granules, and the pH-dependent fluorescence of pHluorin was retained. The NPY-pHluorin fusion protein exploits the granule luminal pH changes that occur during exocytosis to visualize exocytotic events of live islet cells in real time with high spatial resolution in three dimensions[82].

Statistical analysis. All measurements were taken from distinct samples. Means among three or more groups were compared by analysis of variance (ANOVA) in GraphPad Prism 8 software. If deemed significant, Tukey's post-hoc pairwise comparisons were performed. Means between two groups were compared by two-tailed Student's *t*-test. Variances between two groups were compared by *F*-test. A confidence level of 95% was considered significant. The statistical test used, exact *P* values and definition of *n* are all indicated in the individual figure legends. All error bars in the figures display the mean ± s.e.m.

Reagents. The following antibodies were used for immunofluorescence staining:

gp-anti-insulin (Linco no. 4011-01), gp-anti-insulin (Dako no. A0564), ck-anti-insulin (Abcam no. ab14042), sh-anti-glucagon (Abcam no. ab36232), sh-anti-somatostatin (Abcam no. ab35425), rb-anti-pancreatic polypeptide (Abcam no. ab113694), rb-anti-GABA (Sigma-Aldrich no. A2052), ms-anti-GAD65 C-term[109] (in-house RRID:AB_528264), ms-anti-GAD65 N-term[110] (Christiane Hampe Laboratory), rb-anti-GAD65 (Synapic Systems no. 198102), gp-anti-GAD65

(Synaptic Systems no. 198104), rb-anti-TauT (Sigma-Aldrich no. HPA015028), rb-anti-VGAT Oyster 650-labeled (Synaptic Systems no. 131103C5), rb-anti-synaptophysin (Abcam no. ab14692), rb-anti-SV2C (Synaptic Systems no. 119202), rb-anti-4F2HC (Santa Cruz no. sc9160), ms-anti-LAT2 (OriGene no. UM500058), rb-anti-Bestrophin 1 (Abcam no. ab14928), rb-anti-GAT1 (Synaptic Systems no. 274102), rb-anti-GAT2 (Abcam no. ab2896), rb-anti-GAT3 (Synaptic Systems no. 274303), rb-anti-GCP60 (Novus Biologicals no. NBP1-83379), rb-anti-taurine (Sigma-Aldrich no. AB5022) and Alexa Fluor conjugated secondary antibodies (Thermo Fisher).

The following antibodies were used for western blotting:

rb-anti-LRRC8A (Cell Signaling no. 24979), ms-anti-beta actin (Sigma-Aldrich no. A1978) and IRDye conjugated secondary antibodies (LI-COR).

Abbreviations: gp, guinea pig; ck, chicken; ms, mouse; rb, rabbit; sh, sheep.

The following chemicals were used:

CGP 55845 hydrochloride (Tocris Bioscience no. 1248/10), γ-vinyl GABA (Tocris no. 0808), L-allylglycine (Sigma-Aldrich no. A7762), SR 95531 hydrobromide (Tocris no. 1262), Niflumic acid (Tocris no. 4112/50), CFTRinh 172 (Tocris no. 3430/10), NNC711 (Tocris no. 1779/10), SNAP 5114 (Tocris no. 1561/10), NNC05-2090 hydrochloride (Tocris no. 2747/10), Tetrabenazine (Tocris no. 2175), Diazoxide (Tocris no. 0964), GABA (Sigma-Aldrich no. A5835), Serotonin (Sigma-Aldrich no. 14927), DIDS (Sigma-Aldrich no. D3514), ^{3}H-GABA (Perkin-Elmer no. NET191250UC), Muscimol (Tocris no. 0289), Liberase TL (Roche no. 05401020001) and Histopaque-1119 (Sigma-Aldrich no. 11191).

Reporting Summary. Further information on research design is available in the Nature Research Reporting Summary linked to this article.

Data availability

The unique biological materials used in the manuscript are available from the corresponding authors upon reasonable request with the exception of those materials that the authors obtained via a materials transfer agreement that prohibits transfer to third parties; these include the GABA biosensor cells (obtainable from K. Kaupmann, Novartis Institute for BioMedical Research, Basal, Switzerland), *LRRC8A*$^{-/-}$ MIN6 cells and *LRRC8A*$^{fl/fl}$ mice (obtainable from R. Sah, Washington University in St. Louis, MO, USA), and NPY-pHluorin (obtainable from H. Gaisano, University of Toronto, Toronto, ON, Canada). Other requests for materials should be addressed to corresponding author A.C. or E.A.P. Source data for Figs. 1–6 and Extended Data Figs. 1, 4, and 5 are provided with the paper. The data that support the findings of this study are available from the corresponding authors upon reasonable request.

Received: 23 May 2018; Accepted: 4 October 2019;
Published online: 15 November 2019

References

1. Kanaani, J. et al. Compartmentalization of GABA synthesis by GAD67 differs between pancreatic beta cells and neurons. *PLoS ONE* **10**, e0117130 (2015).
2. Rorsman, P. et al. Glucose-inhibition of glucagon secretion involves activation of GABA$_A$-receptor chloride channels. *Nature* **341**, 233–236 (1989).
3. Xu, E. et al. Intra-islet insulin suppresses glucagon release via GABA-GABAA receptor system. *Cell Metab.* **3**, 47–58 (2006).
4. Bailey, S. J., Ravier, M. A. & Rutter, G. A. Glucose-dependent regulation of γ-aminobutyric acid (GABA$_A$) receptor expression in mouse pancreatic islet α-cells. *Diabetes* **56**, 320–327 (2007).
5. Fiorina, P. GABAergic system in β-cells: from autoimmunity target to regeneration tool. *Diabetes* **62**, 3674–3676 (2013).
6. Tian, J. et al. γ-Aminobutyric acid regulates both the survival and replication of human β-cells. *Diabetes* **62**, 3760–3765 (2013).
7. Purwana, I. et al. GABA promotes human β-cell proliferation and modulates glucose homeostasis. *Diabetes* **63**, 4197–4205 (2014).
8. Tian, J., Dang, H. & Kaufman, D. L. Combining antigen-based therapy with GABA treatment synergistically prolongs survival of transplanted β-cells in diabetic NOD mice. *PLoS ONE* **6**, e25337 (2011).
9. Tian, J., Dang, H., Middleton, B. & Kaufman, D. L. Clinically applicable GABA receptor positive allosteric modulators promote β-cell replication. *Sci. Rep.* **7**, 374 (2017).
10. Prud'homme, G. J., Glinka, Y. & Wang, Q. Immunological GABAergic interactions and therapeutic applications in autoimmune diseases. *Autoimmun. Rev.* **14**, 1048–1056 (2015).
11. Untereiner, A. et al. GABA promotes β-cell proliferation, but does not overcome impaired glucose homeostasis associated with diet-induced obesity. *FASEB J.* **33**, 3968–3984 (2019).
12. He, S. et al. Rapamycin/GABA combination treatment ameliorates diabetes in NOD mice. *Mol. Immunol.* **73**, 130–137 (2016).
13. Feng, A. L. et al. Paracrine GABA and insulin regulate pancreatic alpha cell proliferation in a mouse model of type 1 diabetes. *Diabetologia* **60**, 1033–1042 (2017).
14. Ben-Othman, N. et al. Long-term GABA administration induces alpha cell-mediated beta-like cell neogenesis. *Cell* **168**, 73–85 e11 (2017).
15. Li, J. et al. Artemisinins target GABA$_A$ receptor signaling and impair α cell identity. *Cell* **168**, 86–100 e115 (2017).
16. Ackermann, A. M., Moss, N. G. & Kaestner, K. H. GABA and artesunate do not induce pancreatic α-to-β cell transdifferentiation in vivo. *Cell Metab.* **28**, 787–792.e3 (2018).
17. van der Meulen, T. et al. Artemether does not turn α cells into β cells. *Cell Metab.* **27**, 218–225.e214 (2018).
18. Barragan, A., Weidner, J. M., Jin, Z., Korpi, E. R. & Birnir, B. GABAergic signalling in the immune system. *Acta Physiol. (Oxf.)* **213**, 819–827 (2015).
19. Mendu, S. K., Bhandage, A., Jin, Z. & Birnir, B. Different subtypes of GABA-A receptors are expressed in human, mouse and rat T lymphocytes. *PLoS ONE* **7**, e42959 (2012).
20. Jin, Z., Mendu, S. K. & Birnir, B. GABA is an effective immunomodulatory molecule. *Amino Acids* **45**, 87–94 (2013).
21. Bjurstom, H. et al. GABA, a natural immunomodulator of T lymphocytes. *J. Neuroimmunol.* **205**, 44–50 (2008).
22. Bhat, R. et al. Inhibitory role for GABA in autoimmune inflammation. *Proc. Natl Acad. Sci. USA* **107**, 2580–2585 (2010).
23. Tian, J. et al. Gamma-aminobutyric acid inhibits T cell autoimmunity and the development of inflammatory responses in a mouse type 1 diabetes model. *J. Immunol.* **173**, 5298–5304 (2004).
24. Kim, J. et al. Differential expression of GAD65 and GAD67 in human, rat, and mouse pancreatic islets. *Diabetes* **42**, 1799–1808 (1993).
25. Kanaani, J., Patterson, G., Schaufele, F., Lippincott-Schwartz, J. & Baekkeskov, S. A palmitoylation cycle dynamically regulates partitioning of the GABA-synthesizing enzyme GAD65 between ER-Golgi and post-Golgi membranes. *J. Cell Sci.* **121**, 437–449 (2008).
26. Braun, M. et al. Regulated exocytosis of GABA-containing synaptic-like microvesicles in pancreatic β-cells. *J. Gen. Physiol.* **123**, 191–204 (2004).
27. Jin, H. et al. Demonstration of functional coupling between gamma-aminobutyric acid (GABA) synthesis and vesicular GABA transport into synaptic vesicles. *Proc. Natl Acad. Sci. USA* **100**, 4293–4298 (2003).
28. Reetz, A. et al. GABA and pancreatic beta-cells: colocalization of glutamic acid decarboxylase (GAD) and GABA with synaptic-like microvesicles suggests their role in GABA storage and secretion. *EMBO J.* **10**, 1275–1284 (1991).
29. Braun, M. et al. Corelease and differential exit via the fusion pore of GABA, serotonin, and ATP from LDCV in rat pancreatic β cells. *J. Gen. Physiol.* **129**, 221–231 (2007).
30. Soltani, N. et al. GABA exerts protective and regenerative effects on islet beta cells and reverses diabetes. *Proc. Natl Acad. Sci. USA* **108**, 11692–11697 (2011).
31. Braun, M. et al. γ-aminobutyric acid (GABA) is an autocrine excitatory transmitter in human pancreatic β-cells. *Diabetes* **59**, 1694–1701 (2010).
32. Bansal, P. et al. GABA coordinates with insulin in regulating secretory function in pancreatic INS-1 β-cells. *PLoS ONE* **6**, e26225 (2011).
33. Smismans, A., Schuit, F. & Pipeleers, D. Nutrient regulation of gamma-aminobutyric acid release from islet beta cells. *Diabetologia* **40**, 1411–1415 (1997).
34. Wang, C., Mao, R., Van de Casteele, M., Pipeleers, D. & Ling, Z. Glucagon-like peptide-1 stimulates GABA formation by pancreatic beta-cells at the level of glutamate decarboxylase. *Am. J. Physiol. Endocrinol. Metab.* **292**, E1201–E1206 (2007).
35. Garry, D. J., Sorenson, R. L. & Coulter, H. D. Ultrastructural localization of gamma amino butyric acid immunoreactivity in B cells of the rat pancreas. *Diabetologia* **30**, 115–119 (1987).
36. Semyanov, A., Walker, M. C. & Kullmann, D. M. GABA uptake regulates cortical excitability via cell type-specific tonic inhibition. *Nat. Neurosci.* **6**, 484–490 (2003).
37. Garry, D. J., Sorenson, R. L., Elde, R. P., Maley, B. E. & Madsen, A. Immunohistochemical colocalization of GABA and insulin in beta-cells of rat islet. *Diabetes* **35**, 1090–1095 (1986).
38. Kanaani, J., Diacovo, M. J., El-Husseini Ael, D., Bredt, D. S. & Baekkeskov, S. Palmitoylation controls trafficking of GAD65 from Golgi membranes to axon-specific endosomes and a Rab5a-dependent pathway to presynaptic clusters. *J. Cell Sci.* **117**, 2001–2013 (2004).
39. Kanaani, J. et al. A combination of three distinct trafficking signals mediates axonal targeting and presynaptic clustering of GAD65. *J. Cell Biol.* **158**, 1229–1238 (2002).
40. Chaudhry, F. A. et al. The vesicular GABA transporter, VGAT, localizes to synaptic vesicles in sets of glycinergic as well as GABAergic neurons. *J. Neurosci.* **18**, 9733–9750 (1998).
41. Jenstad, M. & Chaudhry, F. A. The amino acid transporters of the glutamate/GABA-glutamine cycle and their impact on insulin and glucagon secretion. *Front. Endocrinol. (Lausanne)* **4**, 199 (2013).
42. Gammelsaeter, R. Glycine, GABA and their transporters in pancreatic islets of Langerhans: evidence for a paracrine transmitter interplay. *J. Cell Sci.* **117**, 3749–3758 (2004).

43. Cabrera, O. et al. Glutamate is a positive autocrine signal for glucagon release. *Cell Metab.* **7**, 545–554 (2008).
44. Rodriguez-Diaz, R. et al. Alpha cells secrete acetylcholine as a non-neuronal paracrine signal priming beta cell function in humans. *Nat. Med.* **17**, 888–892 (2011).
45. Rodriguez-Diaz, R. et al. Real-time detection of acetylcholine release from the human endocrine pancreas. *Nat. Protoc.* **7**, 1015–1023 (2012).
46. Franek, M. et al. The heteromeric GABA-B receptor recognizes G-protein α subunit C-termini. *Neuropharmacology* **38**, 1657–1666 (1999).
47. Pagano, A. et al. C-terminal interaction is essential for surface trafficking but not for heteromeric assembly of $GABA_B$ receptors. *J. Neurosci.* **21**, 1189–1202 (2001).
48. Tengholm, A. & Gylfe, E. Oscillatory control of insulin secretion. *Mol. Cell. Endocrinol.* **297**, 58–72 (2009).
49. Allen, N. J., Káradóttir, R. & Attwell, D. Reversal or reduction of glutamate and GABA transport in CNS pathology and therapy. *Pflugers Arch.* **449**, 132–142 (2004).
50. Richerson, G. B. & Wu, Y. Dynamic equilibrium of neurotransmitter transporters: not just for reuptake anymore. *J. Neurophysiol.* **90**, 1363–1374 (2003).
51. Tian, N. et al. The role of the synthetic enzyme GAD65 in the control of neuronal γ-aminobutyric acid release. *Proc. Natl Acad. Sci. USA* **96**, 12911–12916 (1999).
52. Patel, A. B., de Graaf, R. A., Martin, D. L., Battaglioli, G. & Behar, K. L. Evidence that GAD65 mediates increased GABA synthesis during intense neuronal activity in vivo. *J. Neurochem.* **97**, 385–396 (2006).
53. Wang, C., Ling, Z. & Pipeleers, D. Comparison of cellular and medium insulin and GABA content as markers for living β-cells. *Am. J. Physiol. Endocrinol. Metab.* **288**, E307–E313 (2005).
54. Baron, M. et al. A single-cell transcriptomic map of the human and mouse pancreas reveals inter- and intra-cell population structure. *Cell Syst.* **3**, 346–360.e4 (2016).
55. Wang, Y. J. et al. Single-cell transcriptomics of the human endocrine pancreas. *Diabetes* **65**, 3028–3038 (2016).
56. Grun, D. et al. De novo prediction of stem cell identity using single-cell transcriptome data. *Cell Stem Cell* **19**, 266–277 (2016).
57. Tomi, M., Tajima, A., Tachikawa, M. & Hosoya, K. Function of taurine transporter (Slc6a6/TauT) as a GABA transporting protein and its relevance to GABA transport in rat retinal capillary endothelial cells. *Biochim. Biophys. Acta* **1778**, 2138–2142 (2008).
58. Yahara, T., Tachikawa, M., Akanuma, S., Kubo, Y. & Hosoya, K. Amino acid residues involved in the substrate specificity of TauT/SLC6A6 for taurine and γ-aminobutyric acid. *Biol. Pharm. Bull.* **37**, 817–825 (2014).
59. del Amo, E. M., Urtti, A. & Yliperttula, M. Pharmacokinetic role of L-type amino acid transporters LAT1 and LAT2. *Eur. J. Pharm. Sci.* **35**, 161–174 (2008).
60. Lee, S. et al. Channel-mediated tonic GABA release from glia. *Science* **330**, 790–796 (2010).
61. Voss, F. K. et al. Identification of LRRC8 heteromers as an essential component of the volume-regulated anion channel VRAC. *Science* **344**, 634–638 (2014).
62. Lutter, D., Ullrich, F., Lueck, J. C., Kempa, S. & Jentsch, T. J. Selective transport of neurotransmitters and modulators by distinct volume-regulated LRRC8 anion channels. *J. Cell Sci.* **130**, 1122–1133 (2017).
63. Syeda, R. et al. LRRC8 proteins form volume-regulated anion channels that sense ionic strength. *Cell* **164**, 499–511 (2016).
64. Qiu, Z. et al. SWELL1, a plasma membrane protein, is an essential component of volume-regulated anion channel. *Cell* **157**, 447–458 (2014).
65. Planells-Cases, R. et al. Subunit composition of VRAC channels determines substrate specificity and cellular resistance to Pt-based anti-cancer drugs. *EMBO J.* **34**, 2993–3008 (2015).
66. Kinard, T. A. & Satin, L. S. An ATP-sensitive Cl^- channel current that is activated by cell swelling, cAMP, and glyburide in insulin-secreting cells. *Diabetes* **44**, 1461–1466 (1995).
67. Kang, C. et al. SWELL1 is a glucose sensor regulating β-cell excitability and systemic glycaemia. *Nat. Commun.* **9**, 367. (2018).
68. Stuhlmann, T., Planells-Cases, R. & Jentsch, T. J. LRRC8/VRAC anion channels enhance β-cell glucose sensing and insulin secretion. *Nat. Commun.* **9**, 1974 (2018).
69. Zhang, Y. et al. SWELL1 is a regulator of adipocyte size, insulin signalling and glucose homeostasis. *Nat. Cell Biol.* **19**, 504–517 (2017).
70. Thorens, B. et al. *Ins1*^{Cre} knock-in mice for beta cell-specific gene recombination. *Diabetologia* **58**, 558–565 (2015).
71. Korol, S. V. et al. Functional characterization of native, high-affinity $GABA_A$ receptors in human pancreatic β cells. *EBioMedicine* **30**, 273–282 (2018).
72. Chang, Y., Ghansah, E., Chen, Y., Ye, J. & Weiss, D. S. Desensitization mechanism of GABA receptors revealed by single oocyte binding and receptor function. *J. Neurosci.* **22**, 7982–7990 (2002).
73. Ekholm, R., Ericson, L. E. & Lundquist, I. Monoamines in the pancreatic islets of the mouse. Subcellular localization of 5-hydroxytryptamine by electron microscopic autoradiography. *Diabetologia* **7**, 339–348 (1971).
74. Hutton, J. C., Peshavaria, M. & Tooke, N. E. 5-Hydroxytryptamine transport in cells and secretory granules from a transplantable rat insulinoma. *Biochem. J.* **210**, 803–810 (1983).
75. Kennedy, R. T., Huang, L., Atkinson, M. A. & Dush, P. Amperometric monitoring of chemical secretions from individual pancreatic beta-cells. *Anal. Chem.* **65**, 1882–1887 (1993).
76. Barbosa, R. et al. Real time electrochemical detection of 5-HT/insulin secretion from single pancreatic islets: effect of glucose and K+ depolarization. *Biochem. Biophys. Res. Commun.* **228**, 100–104 (1996).
77. Barbosa, R. et al. Control of pulsatile 5-HT/insulin secretion from single mouse pancreatic islets by intracellular calcium dynamics. *J. Physiol.* **510**(Pt 1), 135–143 (1998).
78. Huang, Y. J. et al. Mouse taste buds use serotonin as a neurotransmitter. *J. Neurosci.* **25**, 843–847 (2005).
79. Almaca, J. et al. Human beta cells produce and release serotonin to inhibit glucagon secretion from alpha cells. *Cell Rep.* **17**, 3281–3291 (2016).
80. Dishinger, J. F., Reid, K. R. & Kennedy, R. T. Quantitative monitoring of insulin secretion from single islets of Langerhans in parallel on a microfluidic chip. *Anal. Chem.* **81**, 3119–3127 (2009).
81. Deeney, J. T., Bränström, R., Corkey, B. E., Larsson, O. & Berggren, P. O. ^{3}H-serotonin as a marker of oscillatory insulin secretion in clonal β-cells (INS-1). *FEBS Lett.* **581**, 4080–4084 (2007).
82. Makhmutova, M., Liang, T., Gaisano, H., Caicedo, A. & Almaca, J. Confocal imaging of neuropeptide Y-pHluorin: a technique to visualize insulin granule exocytosis in intact murine and human islets. *J. Vis. Exp.* **127**, e56089 (2017).
83. Almaca, J. et al. Spatial and temporal coordination of insulin granule exocytosis in intact human pancreatic islets. *Diabetologia* **58**, 2810–2818 (2015).
84. Phelps, E. A. et al. Aberrant accumulation of the diabetes autoantigen GAD65 in Golgi membranes in conditions of ER stress and autoimmunity. *Diabetes* **65**, 2686–2699 (2016).
85. Kass, I. et al. Cofactor-dependent conformational heterogeneity of GAD65 and its role in autoimmunity and neurotransmitter homeostasis. *Proc. Natl Acad. Sci. USA* **111**, E2524–E2529 (2014).
86. Martin, D. L. & Rimvall, K. Regulation of γ-aminobutyric acid synthesis in the brain. *J. Neurochem.* **60**, 395–407 (1993).
87. Chessler, S. D., Simonson, W. T., Sweet, I. R. & Hammerle, L. P. Expression of the vesicular inhibitory amino acid transporter in pancreatic islet cells: distribution of the transporter within rat islets. *Diabetes* **51**, 1763–1771 (2002).
88. Thomas-Reetz, A. C. & De Camilli, P. A role for synaptic vesicles in non-neuronal cells: clues from pancreatic beta cells and from chromaffin cells. *FASEB J.* **8**, 209–216 (1994).
89. Wendt, A. et al. Glucose inhibition of glucagon secretion from rat alpha-cells is mediated by GABA released from neighboring beta-cells. *Diabetes* **53**, 1038–1045 (2004).
90. Braun, M. et al. Corelease and differential exit via the fusion pore of GABA, serotonin, and ATP from LDCV in rat pancreatic β cells. *J. Gen. Physiol.* **129**, 221–231 (2007).
91. Jo, J., Choi, M. Y. & Koh, D. S. Beneficial effects of intercellular interactions between pancreatic islet cells in blood glucose regulation. *J. Theor. Biol.* **257**, 312–319 (2009).
92. Koeslag, J. H., Saunders, P. T. & Terblanche, E. A reappraisal of the blood glucose homeostat which comprehensively explains the type 2 diabetes mellitus-syndrome X complex. *J. Physiol.* **549**, 333–346 (2003).
93. Braun, M. et al. Voltage-gated ion channels in human pancreatic β-cells: electrophysiological characterization and role in insulin secretion. *Diabetes* **57**, 1618–1628 (2008).
94. Gassmann, M. & Bettler, B. Regulation of neuronal GABA(B) receptor functions by subunit composition. *Nat. Rev. Neurosci.* **13**, 380–394 (2012).
95. Farrant, M. & Nusser, Z. Variations on an inhibitory theme: phasic and tonic activation of GABA(A) receptors. *Nat. Rev. Neurosci.* **6**, 215–229 (2005).
96. Braun, M., Ramracheya, R. & Rorsman, P. Autocrine regulation of insulin secretion. *Diabetes Obes. Metab.* **14**(Suppl. 3), 143–151 (2012).
97. Taneera, J. et al. γ-Aminobutyric acid (GABA) signalling in human pancreatic islets is altered in type 2 diabetes. *Diabetologia* **55**, 1985–1994 (2012).
98. Campbell-Thompson, M. et al. Network for Pancreatic Organ Donors with Diabetes (nPOD): developing a tissue biobank for type 1 diabetes. *Diabetes Metab. Res. Rev.* **28**, 608–617 (2012).
99. Pugliese, A. et al. The Juvenile Diabetes Research Foundation Network for Pancreatic Organ Donors with Diabetes (nPOD) Program: goals, operational model and emerging findings. *Pediatr. Diabetes* **15**, 1–9 (2014).
100. Phelps, E. A. et al. Advances in pancreatic islet monolayer culture on glass surfaces enable super-resolution microscopy and insights into beta cell ciliogenesis and proliferation. *Sci. Rep.* **7**, 45961 (2017).

101. Codazzi, F. et al. Synergistic control of protein kinase Cγ activity by ionotropic and metabotropic glutamate receptor inputs in hippocampal neurons. *J. Neurosci.* **26**, 3404–3411 (2006).
102. Bolte, S. & Cordelieres, F. P. A guided tour into subcellular colocalization analysis in light microscopy. *J. Microsc.* **224**, 213–232 (2006).
103. L. Lun, A. T., Bach, K. & Marioni, J. C. Pooling across cells to normalize single-cell RNA sequencing data with many zero counts. *Genome Biol.* **17**, 75 (2016).
104. Dvoryanchikov, G., Huang, Y. A., Barro-Soria, R., Chaudhari, N. & Roper, S. D. GABA, its receptors, and GABAergic inhibition in mouse taste buds. *J. Neurosci.* **31**, 5782–5791 (2011).
105. Cabrera, O. et al. The unique cytoarchitecture of human pancreatic islets has implications for islet cell function. *Proc. Natl Acad. Sci. USA* **103**, 2334–2339 (2006).
106. Rasouli, M. Basic concepts and practical equations on osmolality: biochemical approach. *Clin. Biochem.* **49**, 936–941 (2016).
107. Zandy, S. L., Doherty, J. M., Wibisono, N. D. & Gonzales, R. A. High sensitivity HPLC method for analysis of in vivo extracellular GABA using optimized fluorescence parameters for *o*-phthalaldehyde (OPA)/sulfite derivatives. *J. Chromatogr. B* **1055–1056**, 1–7 (2017).
108. Fernandez, N. A., Liang, T. & Gaisano, H. Y. Live pancreatic acinar imaging of exocytosis using syncollin-pHluorin. *Am. J. Physiol. Cell Physiol.* **300**, C1513–C1523 (2011).
109. Chang, Y. C. & Gottlieb, D. I. Characterization of the proteins purified with monoclonal antibodies to glutamic acid decarboxylase. *J. Neurosci.* **8**, 2123–2130 (1988).
110. Hampe, C. S. et al. A novel monoclonal antibody specific for the N-terminal end of GAD65. *J. Neuroimmunol.* **113**, 63–71 (2001).

Acknowledgements

This work was funded by the Intramural Research Program of UF's Wertheim College of Engineering and J. Crayton Pruitt Family Department of Biomedical Engineering (E.A.P.), the Intramural Research Program of EPFL's School of Life Sciences (S.B.), the Diabetes Research Institute Foundation, NIH grant nos. R56DK084321 (A.C.), R01DK084321 (A.C.) and R01DK106009 (R.S.), the NIDDK-supported Human Islet Research Network (HIRN, RRID:SCR_014393; https://hirnetwork.org; grant no. UC4DK104208 (E.A.P)), a JDRF award (grant no. 31-2008-416) to the European Consortium for Islet Transplantation (ECIT) Islets for Basic Research Program, a JDRF Faculty Transition Award (grant no. 1-FAC-2017-367-A-N) (E.A.P.), a JDRF Advanced Postdoctoral Fellowship (grant no. 3-APF-2014-208-A-N) (E.A.P.), a Whitaker International Program Postdoctoral Scholarship (E.A.P.), The Shepard Broad Foundation (E.A.P.), the Swedish Research Council (P.-O.B.), the Novo Nordisk Foundation (P.-O.B.), the Family Erling-Persson Foundation (P.-O.B.), the Stichting af Jochnick Foundation (P.-O.B.), the American Diabetes Association (grant no. 1-18-IBS-229) (R.S.) and the Canadian Institutes for Health Research (grant nos. PJT-159741 and PJT-148652) (H.Y.G.).

Human pancreatic islets were provided by the NIDDK-funded Integrated Islet Distribution Program (IIDP) at City of Hope, NIH grant no. 2UC4DK098085, and the JDRF-funded IIDP Islet Award Initiative (E.A.P.). This research was performed with the support of the Network for Pancreatic Organ donors with Diabetes (nPOD; RRID:SCR_014641), a collaborative type 1 diabetes research project sponsored by JDRF (grant no. 5-SRA-2018-557-Q-R) and The Leona M. & Harry B. Helmsley Charitable Trust (grant no. 2018PG-T1D053). The content and views expressed are the responsibility of the authors and do not necessarily reflect the official view of nPOD. Organ Procurement Organizations (OPO) partnering with nPOD to provide research resources are listed at http://www.jdrfnpod.org/for-partners/npod-partners/. The work with human pancreatic sections and islets was also made possible by the Human Islet Cell Processing Facility at the Diabetes Research Institute (University of Miami) and ECIT.

We wish to extend our thanks to the following individuals: D. Bosco and T. Berney, University of Geneva, and L. Piemonti, San Raffaele Scientific Institute, Milan, for human islets through ECIT; C. Mathews, University of Florida, and R. Bottino, Institute of Cellular Therapeutics, Allegheny Health Network, Pittsburgh, Pennsylvania, for human islets through the nPOD Islet Isolation Program; K. Kaupmann, Novartis Institutes for BioMedical Research, Switzerland, for providing the genetically modified GABA biosensor CHO cells; and S. D. Roper for conceptual input on the biosensor cell approach and for critically reading the manuscript; J. Hubbell and M. Swartz, EPFL and University of Chicago, for support; C. Rancourt, University of Florida, for mouse colony management; and M. Pasquier, K. Johnson, B. Benjamin, D. Garcia, P. Parente, A. Arzu, L. Barash, M. Formoso, R. Arrojo e Drigo and A. Tamayo for technical assistance.

Author contributions

E.A.P. and S.B. conceived and carried out subcellular studies of GABA-ergic components in islet cells. D.M. and A.C. conceived and identified GABA release from islets in pulses and pioneered the biosensor cell technique for analyzing the dynamics of islet GABA release. E.A.P. conceived and identified the role of VRAC and TauT in GABA release and uptake. D.W.H. and E.A.P. analyzed the genetic models for *LRRC8A*$^{-/-}$ MIN6 cells, βc-*LRRC8A*$^{-/-}$ murine islets and knock-down LRRC8A-shRNA human islets. D.M., D.W.H. and E.A.P. performed experiments to detect GABA, taurine and serotonin/insulin secretion. J.M. and J.A. performed hormone assay experiments and ELISAs. J.A. conducted NPY-pHluorin experiments to measure exocytosis. H.Y.G. generated adeno-NPY-pHluorin vectors. R.S. generated genetic models for *LRRC8A*$^{-/-}$ MIN6 cells and *LRRC8A*$^{fl/fl}$ murine islets. C.K. isolated and shipped *LRRC8A*$^{fl/fl}$ murine islets. M.W.B. isolated rodent islets and performed western blot analyses. C.C. prepared cultures of primary rat hippocampal neurons. P.C.S. performed bioinformatics analysis. R.N. and F.L. isolated human islets for research. E.A.P., D.M., D.W.H., J.A., C.C., R.M.D. and R.R.-D. collected, analyzed and quantified immunohistochemical data. P.-O.B. provided critical equipment, reagents, expertise and support. D.M., D.W.H., S.B., A.C. and E.A.P. designed the study, analyzed data and wrote the paper. All authors discussed the results and commented on the manuscript.

Competing interests

The authors declare no competing interests.

Additional information

Extended data is available for this paper at https://doi.org/10.1038/s42255-019-0135-7.

Supplementary information is available for this paper at https://doi.org/10.1038/s42255-019-0135-7.

Correspondence and requests for materials should be addressed to S.B., A.C. or E.A.P.

Peer review information Primary Handling Editor: Ana Mateus.

Reprints and permissions information is available at www.nature.com/reprints.

Publisher's note Springer Nature remains neutral with regard to jurisdictional claims in published maps and institutional affiliations.

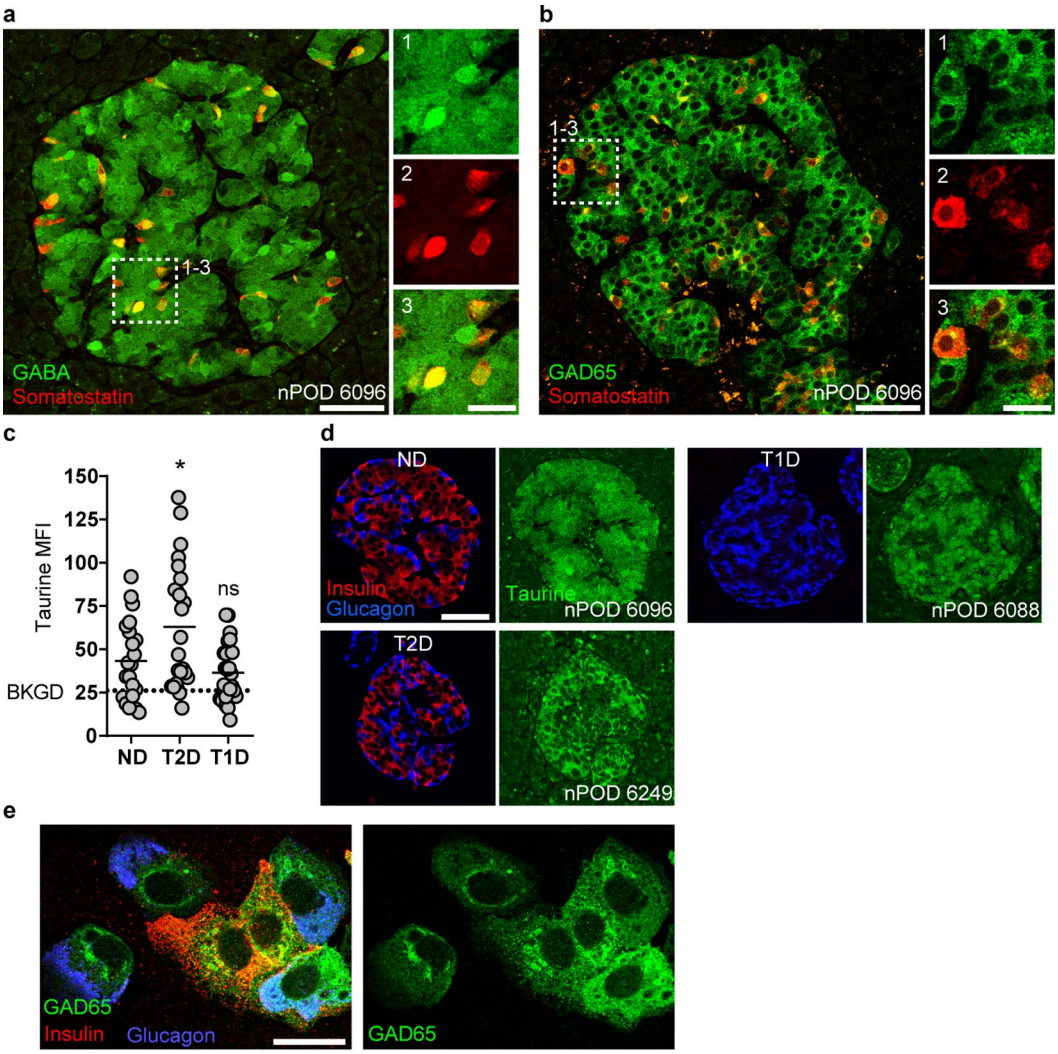

Extended Data Fig. 1 | Delta cells in human islets contain GABA and express GAD65; taurine content is preserved in diabetic islets. a-b. Islets in a non-diabetic human pancreas immunostained for GABA and somatostatin (**a**); or GAD65 and somatostatin (**b**). GABA and GAD65 are present in somatostatin producing human delta cells. Scale bar 50 μm. Right panels show higher magnification views of the boxed region showing channels for: (**a**) (1) GABA only, (2) somatostatin only, and (3) GABA and somatostatin; (**b**) (1) GAD65 only, (2) somatostatin only, and (3) GAD65 and somatostatin. Images are representative of data plotted in Figures 1b and 1j. Scale bar 20 μm. **c**. Quantification of taurine mean fluorescence intensity (MFI) per islet in confocal images of human pancreas sections from non-diabetic (n = 21 islets, 6 donors), type 2 diabetic (n = 24 islets, 8 donors), and type 1 diabetic donors (n = 24 islets, 8 donors). Background (BKGD) indicates average taurine MFI in acinar tissue outside of the islet. One-way ANOVA: ND vs. T2D (*$P = 0.0430$), ND vs. T1D (ns, $P = 0.6667$). Center line indicates the mean. **d**. Human pancreas sections immunostained for taurine, insulin, and glucagon from a non-diabetic, type 2 diabetic and, type 1 diabetic donor. Left panels show insulin and glucagon channels, while right panels show taurine channel from the same image. Images are representative of the dataset plotted in panel c. Scale bars 50 μm. **e**. Representative confocal image of a monolayer of human islet endocrine cells showing immunostaining for GAD65, insulin, and glucagon (left panel) and GAD65 alone (right panel). Images are representative of 3 human islet preparations. Scale bar 20 μm.

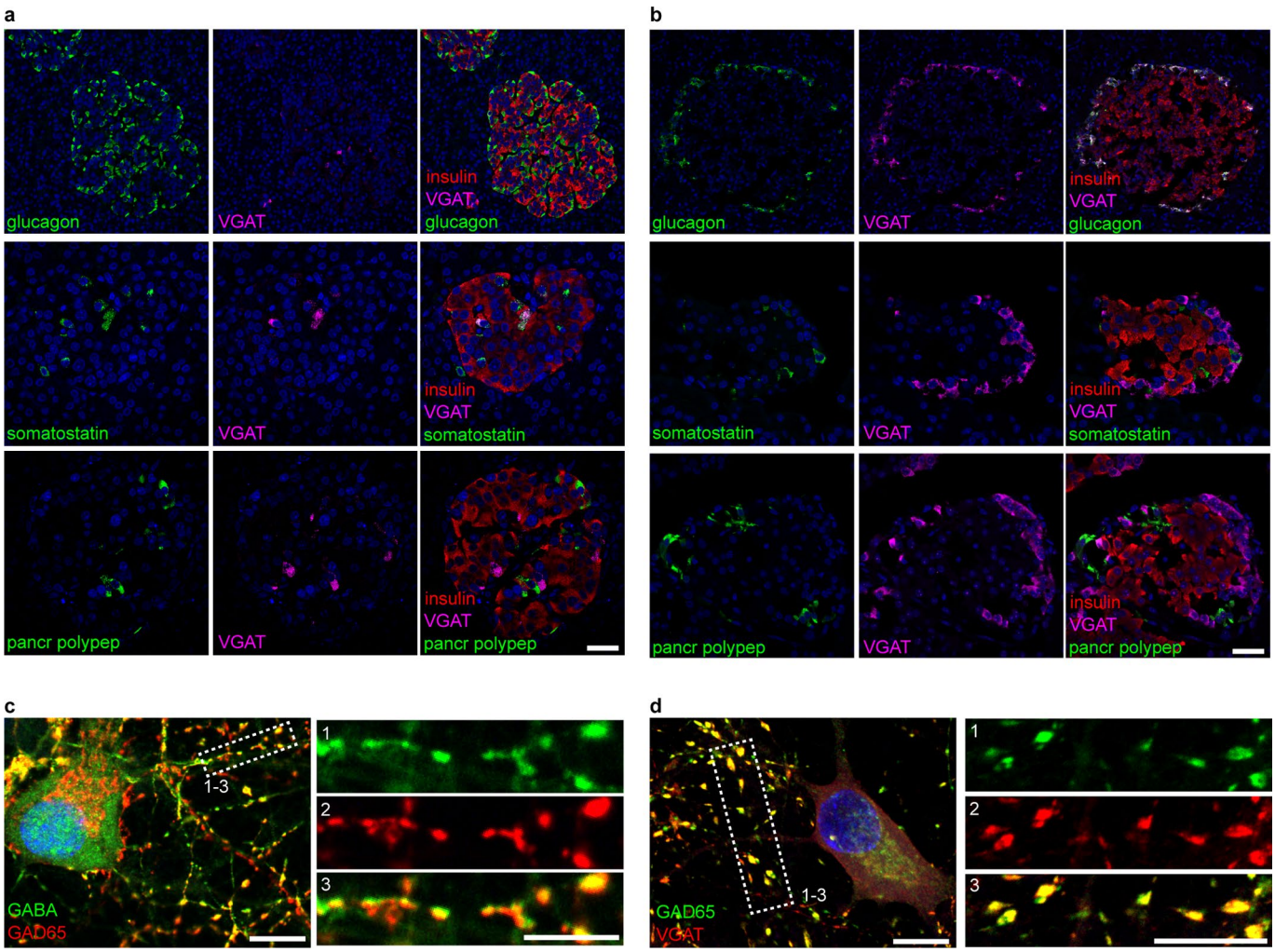

Extended Data Fig. 2 | VGAT expression is concentrated in delta cells of human islets and alpha cells of rat islets; GABA colocalizes with GAD65 and VGAT in synaptic vesicles in neurons. a-b. Islets in a non-diabetic human pancreas (**a**) and rat pancreas (**b**) immunostained for VGAT, insulin, glucagon, somatostatin, and pancreatic polypeptide. VGAT is absent in most beta cells but present in somatostatin producing human delta cells and glucagon producing rat alpha cells. Results are representative of the dataset plotted in Figure 1b. Scale bar 50 μm. **c**. Rat hippocampal neuron immunostained for GABA and the GABA biosynthesizing enzyme GAD65. Scale bar 10 μm. Right panels show higher magnification views of the boxed region showing channels for: (1) GABA only; (2) GAD65 only; (3) GABA and GAD65. GAD65 and GABA colocalize in vesicles. Results are representative of n = 3 rat neuron preparations. Scale bar 5 μm. **d**. Rat hippocampal neuron immunostained for GAD65 and the vesicular GABA transporter VGAT, which is present in synaptic vesicle membranes. Scale bar 10 μm. Right panels show higher magnification views of the boxed region showing channels for: (1) GAD65 only; (2) VGAT only; (3) GAD65 and VGAT. GAD65 and VGAT colocalize in synaptic vesicles. Results are representative of n = 3 rat neuron preparations. Scale bar 5 μm.

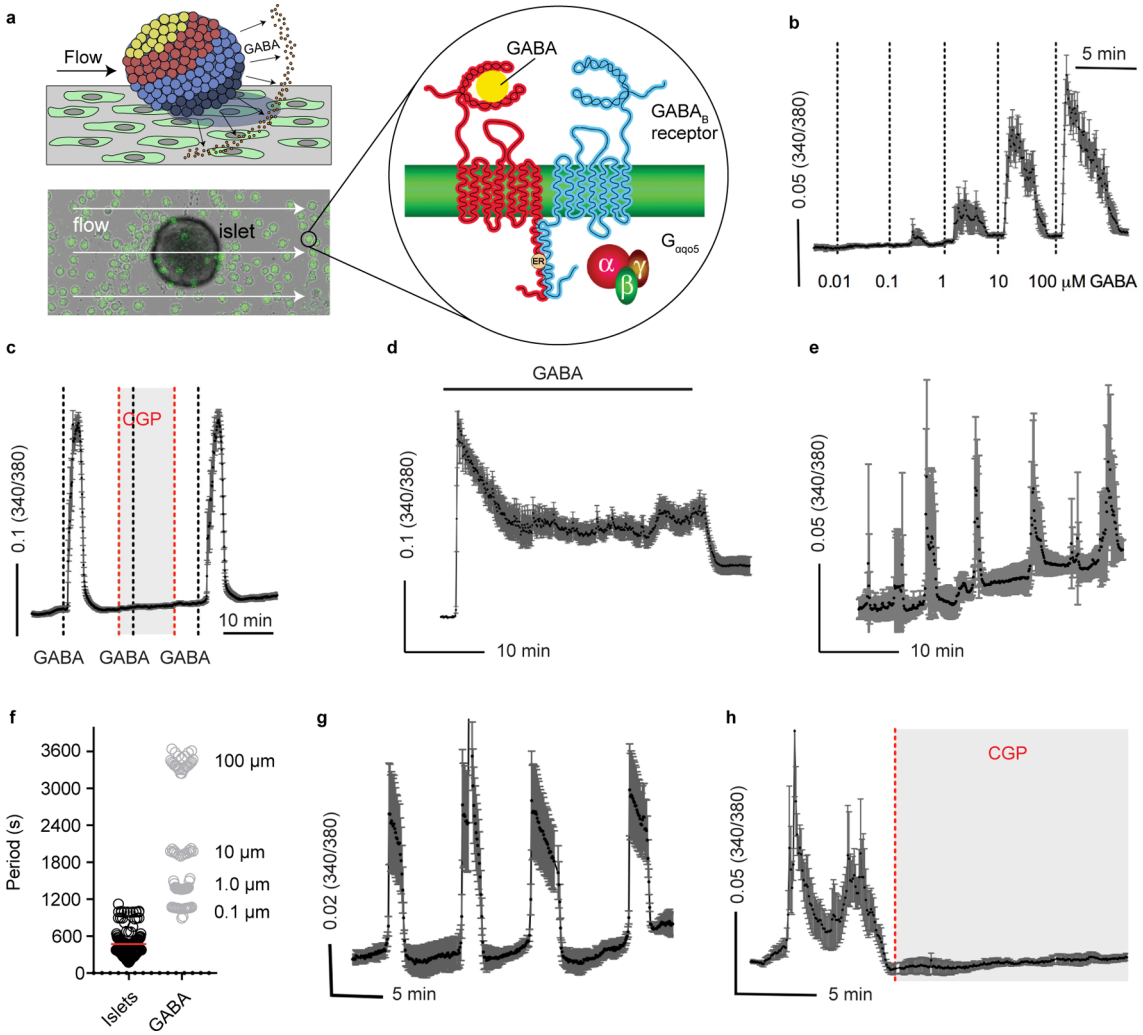

Extended Data Fig. 3 | Characterization of GABA biosensor cells for detecting GABA released from human islets. a. Schematic and image of the GABA biosensor cell assay setup (left panel). Biosensor cells consist of CHO cells stably expressing the heteromeric $GABA_B$ receptor ($GABA_B$ R1b and $GABA_B$ R2) and the G-protein α subunit, Gαqo5 to allow for GABA detection by intracellular Ca^{2+} mobilization ($\Delta[Ca^{2+}]_i$) (right panel). GABA biosensor cells are pre-loaded with the $[Ca^{2+}]_i$ indicator Fura-2 and plated on poly-d-lysine coated cover slips in a perfusion chamber. Individual islets are placed on top of this layer of biosensor cells and connected to a closed bath small volume imaging chamber to ensure linear solution flow and fast exchange. **b**. Titration of exogenous GABA showing concentration-dependence of Ca^{2+} flux in GABA biosensor cells. The plot shows the average 340/380 Fura-2 ratio of n = 5 GABA biosensor cells in the same field of view. Mean ± SEM. **c**. Effect of the selective $GABA_B$ receptor antagonist CGP5584 on biosensor cell responses to exogenously applied GABA. n = 5 biosensor cells in the field of view. Mean ± SEM. **d**. Biosensor cell intracellular Ca^{2+} responses remain elevated during sustained (30 min) exposure to GABA (100 μM shown). n = 5 GABA biosensor cells in the field of view. Mean ± SEM. **e**. GABA release from a human islet maintained in 3 mM glucose. n = 5 GABA biosensor cells located under or immediately downstream of the islet. This is a representative trace of experiments performed on 40 human islet preparations. Mean ± SEM. **f**. Biosensor cells have tonic responses to continuously applied GABA and phasic responses to GABA pulses released from islets. Periods of pulsatile GABA release measured from n = 22 human islet preparations, ≥ 3 islets per preparation (black circles) as shown in panel e. Calculated periods for biosensor cell responses to continuously applied GABA (gray circles) at 0.1, 1, 10, and 100 μM GABA as shown in panel d. Center line indicates the mean. **g**. GABA release from a human islet maintained in 3 mM glucose without addition of inhibitors. n = 5 GABA biosensor cells located under or immediately downstream of the islet. This is a representative trace of experiments performed on 40 human islet preparations. Mean ± SEM. **h**. Effect of the selective $GABA_B$ receptor antagonist CGP5584 on biosensor cell detection of GABA released from a single human islet. n = 5 GABA biosensor cells located under or immediately downstream of the islet. Trace is representative of 3 independent experiments with different human islet preparations. Mean ± SEM.

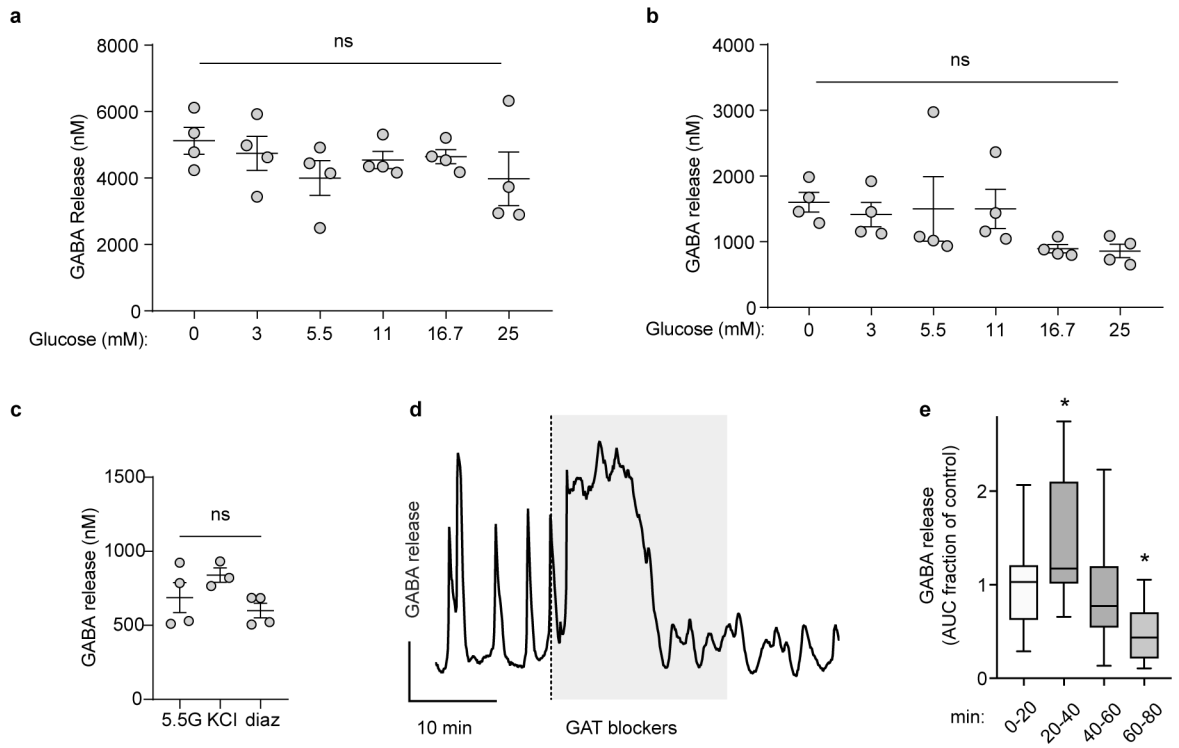

Extended Data Fig. 4 | GABA release does not depend on glucose but is activated by VRAC opening. a-b. Titration of glucose concentrations from 0-25 mM has no effect on islet GABA release. HPLC quantification of GABA released from rat (**a**) and human (**b**) islets during 30 mins static incubation in KRBH of the indicated glucose concentrations. n = 4 samples of 100 islets. One-way ANOVA, $P = 0.5563$ rat (a), $P = 0.2053$ human (**b**), ns = not significant. Mean ± SEM. **c**. HPLC quantification of GABA released from human islets in 5.5 mM glucose (n = 4 samples of 100 human islets), 30 mM KCl (n = 3 samples of 100 human islets), or diazoxide (100 μM) (n = 4 samples of 100 human islets). One-way ANOVA, $P = 0.1511$, ns = not significant. Mean ± SEM. **d**. Effect of the GAT inhibitors SNAP5114 (50 μM), NNC05-2090 (50 μM), and NNC711 (10 μM) on biosensor detection of GABA secretion from a human islet. GAT inhibitors were present throughout the shaded portion of trace. Results are representative of the data plotted in panel **e**. **e**. Quantification of GABA release following treatment with GAT inhibitors. Box extends from 25th to 75th percentiles, center line represents the median, whiskers represent smallest to largest values. n = 3 islets, One-way ANOVA, 0-20 min vs. 20-40 min (*$P = 0.002$), 0-20 min vs. 40-60 min ($P = 0.9194$), 0-20 min vs. 60-80 min (*$P = 0.0058$).

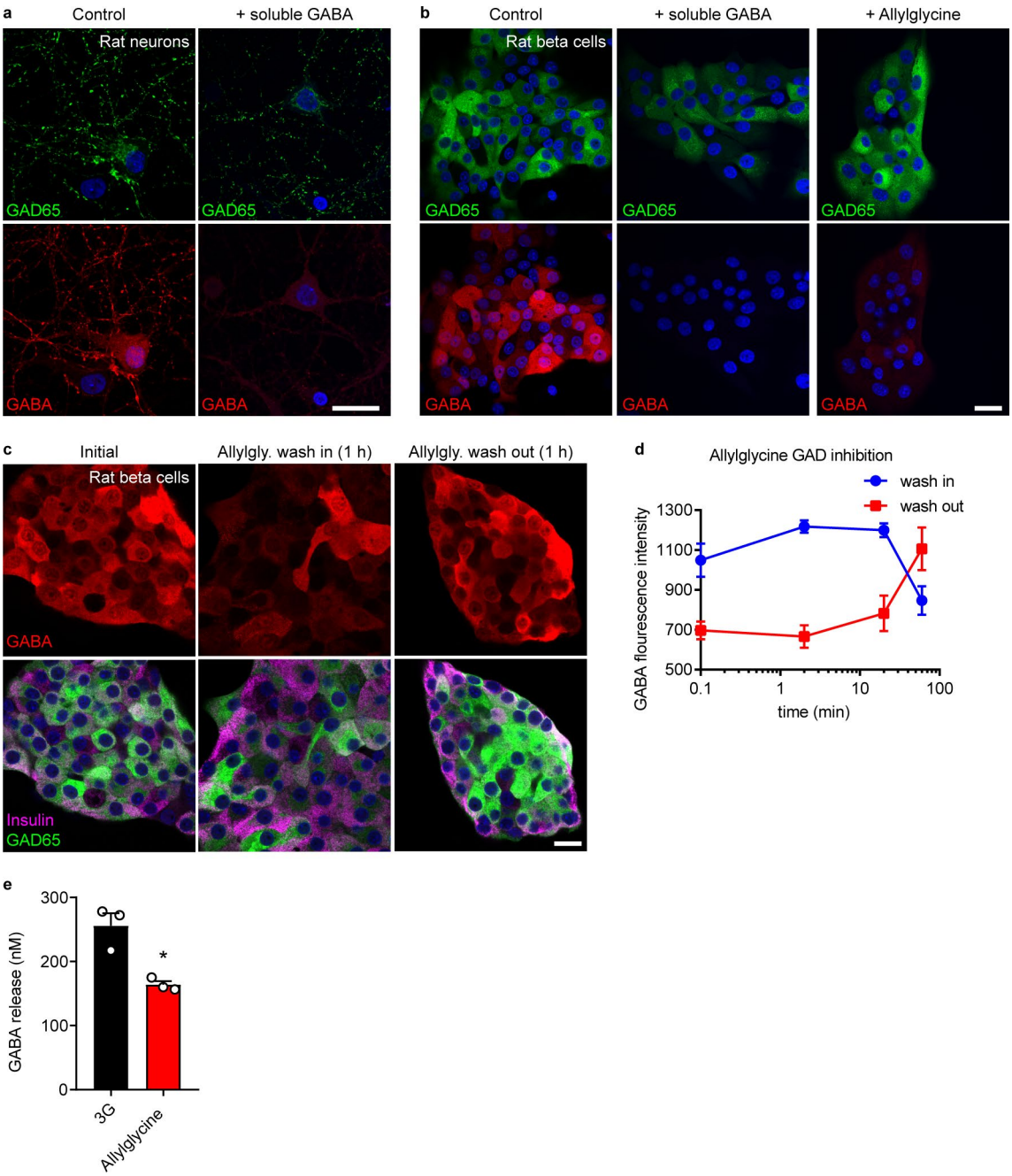

Extended Data Fig. 5 | Allylglycine inhibition of beta cell GABA content and secretion. a-b. Validation of GABA antibody via immunostaining of paraformaldehyde-fixed rat hippocampal neurons (**a**) or rat islet cell monolayers (**b**) for GAD65, GABA, and insulin (not shown) without or with addition of soluble GABA to the primary antibody incubation buffer; or without or with preincubation of cells with allylglycine (10 mM) to inhibit GABA biosynthesis. Images are representative of 3 experimental replicates. Scale bars 20 μm. **c**. Immunostaining of paraformaldehyde-fixed rat islets cell monolayers for GABA, insulin, and GAD65, following allylglycine (10 mM) addition and removal. Images are representative of the dataset plotted in panel d. **d**. Quantification of GABA mean fluorescence intensity (MFI) in rat islet cell monolayers in allylglycine timecourse experiments shown in panel c. n = 4 coverslips. Mean ± SEM. **e**. HPLC analysis of GABA release from human islets during a 30 min addition of allylglycine (no pre-incubation). n = 3 samples of ~100 islets each. Statistical analysis by two-tailed *t*-test, $^*P = 0.0104$. Mean ± SEM.

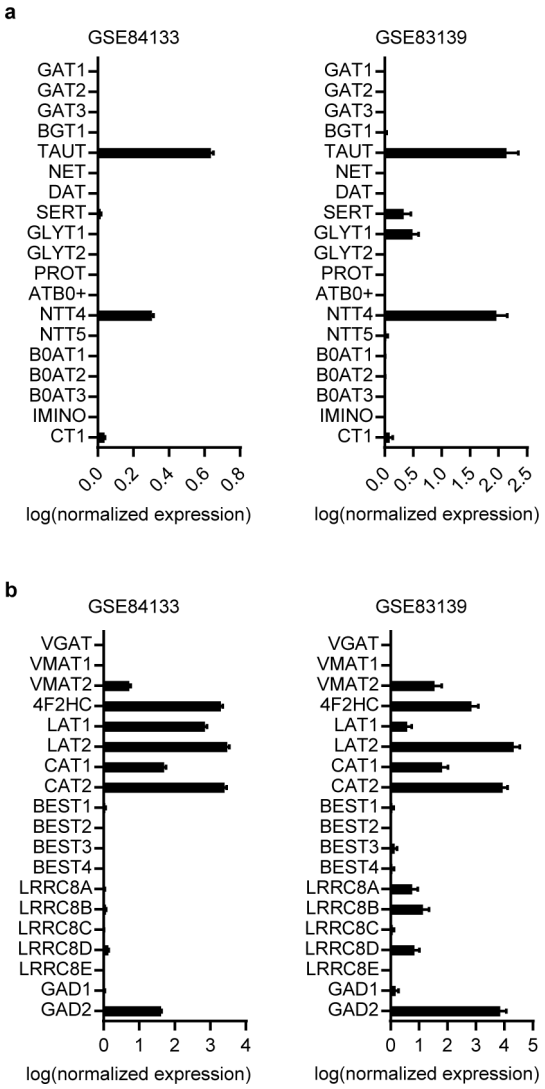

Extended Data Fig. 6 | Human islet single-cell RNA-seq for expression of genes of interest. a. Expression of neurotransmitter transporter family genes (SLC6A). Mean ± SEM. **b**. Expression of genes of interest reported in the literature as related to GABA or putative GABA membrane transporters. Mean ± SEM. Data shown are from two datasets[54,55], but results agree with and are representative of three different curated human single-cell RNA-seq datasets analyzed[54–56] (see also Figure 4).

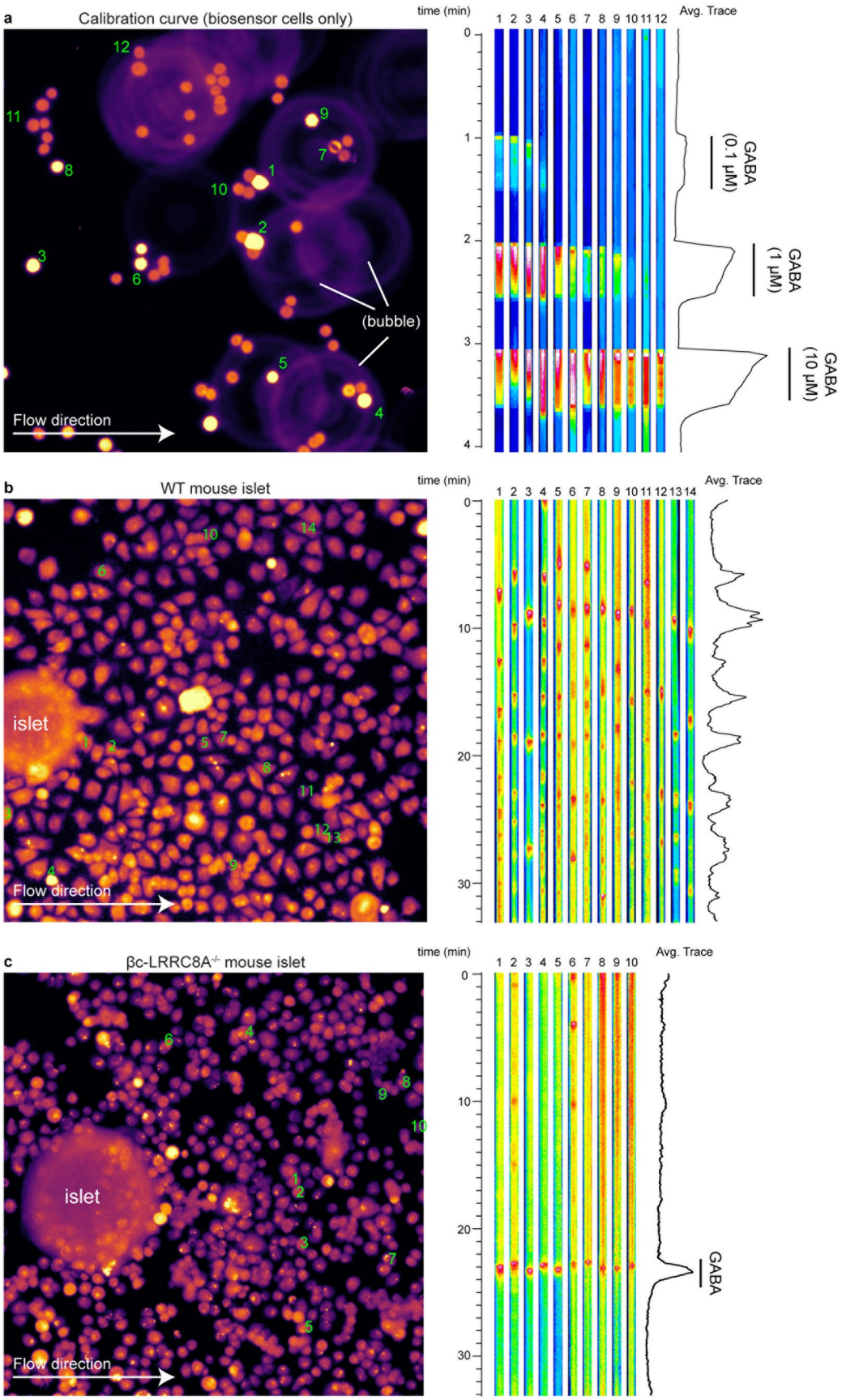

Extended Data Fig. 7 | Kymographs of individual GABA biosensor cells. a-b. Still image, kymographs, and average trace from timelapse videos of Fura-2 $[Ca^{2+}]_i$ signals in GABA biosensor cells in a perfusion flow field in 3 mM glucose isotonic KRBH exposed to (**a**) 0.1, 1, and 10 µM GABA, (**b**) downstream from a wild type mouse islet, and (**c**) downstream from a βc-*LRRC8A*$^{-/-}$ mouse islet. GABA (1 µM) is added to (**c**) at 23 min. GABA-responsive cells were selected for analysis, while unresponsive cells were not analyzed. Data are representative of three independent experiments. See also Supplementary Videos 1–3.

nature research

Corresponding author(s): Steinunn Baekkeskov, Alejandro Caicedo, Edward Phelps

Last updated by author(s): Sep 23, 2019

Reporting Summary

Nature Research wishes to improve the reproducibility of the work that we publish. This form provides structure for consistency and transparency in reporting. For further information on Nature Research policies, see Authors & Referees and the Editorial Policy Checklist.

Statistics

For all statistical analyses, confirm that the following items are present in the figure legend, table legend, main text, or Methods section.

n/a	Confirmed
☐	☒ The exact sample size (*n*) for each experimental group/condition, given as a discrete number and unit of measurement
☐	☒ A statement on whether measurements were taken from distinct samples or whether the same sample was measured repeatedly
☐	☒ The statistical test(s) used AND whether they are one- or two-sided *Only common tests should be described solely by name; describe more complex techniques in the Methods section.*
☐	☒ A description of all covariates tested
☐	☒ A description of any assumptions or corrections, such as tests of normality and adjustment for multiple comparisons
☐	☒ A full description of the statistical parameters including central tendency (e.g. means) or other basic estimates (e.g. regression coefficient) AND variation (e.g. standard deviation) or associated estimates of uncertainty (e.g. confidence intervals)
☐	☒ For null hypothesis testing, the test statistic (e.g. *F*, *t*, *r*) with confidence intervals, effect sizes, degrees of freedom and *P* value noted *Give P values as exact values whenever suitable.*
☒	☐ For Bayesian analysis, information on the choice of priors and Markov chain Monte Carlo settings
☒	☐ For hierarchical and complex designs, identification of the appropriate level for tests and full reporting of outcomes
☒	☐ Estimates of effect sizes (e.g. Cohen's *d*, Pearson's *r*), indicating how they were calculated

Our web collection on statistics for biologists contains articles on many of the points above.

Software and code

Policy information about availability of computer code

Data collection	Confocal microscopy images were acquired with Zeiss Zen v2.3 SP1 (black edition) and Leica Application Suite (LAS) X v3.5.2.18963 software. Fura-2 calcium recordings were acquired with Metafluor software v7.7.3.0 and Zeiss Zen v2.61 (blue edition). Western blots were scanned using LI-COR Image Studio v5.2.
Data analysis	Statistical analysis was performed in Graphpad Prism 8. Images were analyzed with the FIJI distribution of ImageJ (NIH) v1.52p, JACoP (Just Another Colocalization Plugin for ImageJ), v.2.1.1. Single cell RNA-seq analysis was performed in R v3.3.1 and Bioconductor v3.4 with package Scran: methods for single-cell RNA-Seq Analysis v.1.2.2.

For manuscripts utilizing custom algorithms or software that are central to the research but not yet described in published literature, software must be made available to editors/reviewers. We strongly encourage code deposition in a community repository (e.g. GitHub). See the Nature Research guidelines for submitting code & software for further information.

Data

Policy information about availability of data

All manuscripts must include a data availability statement. This statement should provide the following information, where applicable:

- Accession codes, unique identifiers, or web links for publicly available datasets
- A list of figures that have associated raw data
- A description of any restrictions on data availability

The datasets generated and/or analyzed during the current study are available from the corresponding author on reasonable request.

Field-specific reporting

Please select the one below that is the best fit for your research. If you are not sure, read the appropriate sections before making your selection.

☒ Life sciences ☐ Behavioural & social sciences ☐ Ecological, evolutionary & environmental sciences

For a reference copy of the document with all sections, see nature.com/documents/nr-reporting-summary-flat.pdf

Life sciences study design

All studies must disclose on these points even when the disclosure is negative.

Sample size	Sample sizes were chosen based on power analyses taking into account expected variance within and between groups. In other cases (ie. the number of donors tested), the maximum number of (as in all) islet donors we could obtain over the time period of the study were tested. In instances of microscopy image analysis, a power analysis was often not possible as the variance was unknown in advance, thus reasonable sample sizes (value of n is listed on all figure legends) to achieve statistical power were chosen based on the prior experience of the investigators working with this type of data.
Data exclusions	The only data to be excluded from analysis were occasional biosensor cell calcium recordings when there was an insufficient biosensor cell response to allow for data quantification due to ineffective sample preparation. This exclusion criterion was pre-established.
Replication	All attempts at replication were successful. Of note, GABA pulses were replicated by two independent labs using different equipment, islets, and biosensor cells. The glucose-independence of aggregate GABA release was replicated by three different labs. Reproducibility of the experimental findings was verified by three or more independent experiments.
Randomization	Within experiments, islets were aliquoted equally from a stock culture into random individual groups. Coverslips containing monolayer cultures of rat hippocampal neurons from the same tissue preparation were randomly assigned to individual groups.
Blinding	Investigators were blinded to group allocation during data analysis. It was not always possible or practical for investigators to be blinded to donor type (type 2 diabetic, etc) during data collection as human islets were received from one donor at time.

Reporting for specific materials, systems and methods

We require information from authors about some types of materials, experimental systems and methods used in many studies. Here, indicate whether each material, system or method listed is relevant to your study. If you are not sure if a list item applies to your research, read the appropriate section before selecting a response.

Materials & experimental systems

n/a	Involved in the study
☐	☒ Antibodies
☐	☒ Eukaryotic cell lines
☒	☐ Palaeontology
☐	☒ Animals and other organisms
☒	☐ Human research participants
☒	☐ Clinical data

Methods

n/a	Involved in the study
☒	☐ ChIP-seq
☒	☐ Flow cytometry
☒	☐ MRI-based neuroimaging

Antibodies

Antibodies used

The following antibodies were utilized for immunofluorescence staining:
insulin | gp | polyclonal | Linco #4011-01 | 1:10000 | lot No not available
insulin | gp | polyclonal | Dako #A0564 | 1:1000| lot No 10123176
insulin | ck | polyclonal | Abcam #ab14042 | 1:2000 | lot No GR177519-2, GR177519-8
glucagon | sh | polyclonal | Abcam #ab36232 | 1:500 | lot No GR288569-3
somatostatin | sh | polyclonal | Abcam #ab35425 | 1:200 | lot No GR-59464-1
pancreatic polypeptide | rb | polyclonal | Abcam #ab113694 | 1:1000| lot No not available
GABA | rb | polyclonal | Sigma-Aldrich #A2052 | 1:500 | lot No 112M4768, O65M4818V
GAD65 C-term (GAD6) | ms | monoclonal | in-house RRID #AB_2314499 | 1:1000 | lot No not available
GAD65 N-term | ms | monoclonal | Christiane Hampe Lab | 1:300 | lot No not available
GAD65 | rb | polyclonal | Synaptic Systems #198102 | 1:2000 | lot No not available
GAD65 | gp | polyclonal |Synaptic Systems #198104 | 1:500 | lot No not available
TauT | rb | polyclonal | Sigma-Aldrich #HPA015028 | 1:200 | lot No A89837
VGAT Oyster 650-labeled | rb | polyclonal | Synaptic Systems #131103C5 | 1:1000 | lot No 131103C5/1
synaptophysin | rb | polyclonal | Abcam #ab14692 | 1:250 | lot No not available
SV2C | rb | polyclonal | Synaptic Systems #119202 | 1:500 | lot No 11920/4
4F2HC (CD98) | rb | polyclonal | Santa Cruz Biotech #sc9160 | 1:250 | lot No i1014

LAT2 (SLC7A8) | ms | monoclonal, clone #UMAB70 | OriGene #UM500058 | 1:100 | lot No not available
Bestrophin 1 | rb | polyclonal | Abcam #ab14928 | 1:250 | lot No not available
GAT1 | rb | polyclonal | Synaptic Systems #274102 | 1:500 | lot No 274102/1
GAT2 | rb | polyclonal | Abcam #ab2896 | 1:200 | lot No GR139542-1
GAT3 | rb | polyclonal | Synaptic Systems #274303 | 1:500 | lot No 274303/1
GCP60 | rb | polyclonal | Novus Biologicals # NBP1-83379 | 1:500 | lot No not available
taurine | rb | polyclonal | Sigma-Aldrich #AB5022 | 1:100 | lot No 2893310

Alexa Fluor conjugated secondary antibodies (Thermo Fisher)
Goat/Donkey anti-gp/ck/ms/rb/sh IgG (H+L) Highly Cross-Adsorbed Secondary Antibodies, Alexa Fluor 405/488/568/647 | 1:200
Thermo Fisher #A-31553, A-31556, A-11029, A-11034, A-11073, A32931, A-11031, A-11036, A-11075, A-11041, A-21236, A-21245, A-21450, A32933, A-21202, A-21206, A-11015, A10037, A10042, A-21099, A-31571, A-31573, A-21448

The following antibodies were utilized for Western blotting:
LRRC8A | rb | polyclonal | Cell Signaling #24979 | 1:500 | lot No not available
beta actin | ms | monoclonal, clone #AC-15| Sigma-Aldrich #A1978 | 1:10000 | lot No not available

IRDye conjugated secondary antibodies (LI-COR, Inc)
IRDye 800CW Goat anti-Rabbit IgG | LI-COR #926-32211 | 1:10000 | lot No not available
IRDye 680RD Goat anti-Mouse IgG | LI-COR # 926-68070 | 1:40000 | lot No not available

gp = guinea pig, ck = chicken, ms = mouse, rb = rabbit, sh = sheep

Validation

All commercial antibodies were purchased from vendors that included validation and characterization statements on the manufacturer's information sheet. For antibodies that were non-commercial, validation was also performed in previous publications, as referenced in the Methods section. We further conducted extensive validation of the antibody for GABA (Extended Data 6). The commercial LRRC8A antibodies were validated using knockout MIN6 cells and knockout mouse islets.

The following antibodies utilized for immunofluorescence staining were validated as follows:
insulin | gp | Linco #4011-01 | colocalization with second known primary antibody specific for same target, cell-type specificity (beta cells only) in conjunction with glucagon and somatostatin, subcellular localization (insulin granules), western blot single band at expected molecular weight
insulin | gp | Dako #A0564 | colocalization with second known primary antibody specific for same target, cell-type specificity (beta cells only) in conjunction with glucagon and somatostatin, subcellular localization (insulin granules)
insulin | ck | Abcam #ab14042 | colocalization with second known primary antibody specific for same target, cell-type specificity (beta cells only) in conjunction with glucagon and somatostatin, subcellular localization (insulin granules)
glucagon | sh | Abcam #ab36232 | morphology, cell-type specificity (alpha cells only), cell-type specificity (alpha cells only) in conjunction with insulin and somatostatin, subcellular localization (glucagon secretory granules)
somatostatin | sh | Abcam #ab35425 | morphology, cell-type specificity (delta cells only) in conjunction with insulin and glucagon
pancreatic polypeptide | rb | Abcam #ab113694 | morphology / cell-type specificity (PP cells only) in conjunction with insulin and glucagon
GABA | rb | Sigma-Aldrich #A2052 | no non-specific binding with dot blot array of 21 essential amino acids and GABA, no staining in knockout models (cells known not to produce GABA), cell treatment with GABA biosynthesis inhibitor allylglycine, competitive inhibition of binding with soluble GABA, colocalization in neurons with known synaptic vesicle markers
GAD65 C-term (GAD6) | ms | in-house RRID #AB_2314499 | colocalization with second known primary antibody specific for same target, knockout models (cells known not to produce GAD65), morphology and subcellular localization (Golgi + vesicles)
GAD65 N-term | ms | Christiane Hampe Lab | colocalization with second known primary antibody specific for same target, morphology and subcellular localization (Golgi + vesicles), western blot band at expected molecular weight
GAD65 | rb | Synaptic Systems #198102 | colocalization with second known primary antibody specific for same target, morphology and subcellular localization (Golgi + vesicles), vendor validation: immunofluorescence and western blot
GAD65 | gp |Synaptic Systems #198104 | colocalization with second known primary antibody specific for same target, morphology and subcellular localization (Golgi + vesicles), vendor validation: immunofluorescence and western blot
TauT | rb | Sigma-Aldrich #HPA015028 | relied on vendor validation
VGAT Oyster 650-labeled | rb | Synaptic Systems #131103C5 | colocalization in neurons with known synaptic vesicle markers, vendor validation: immunofluorescence
synaptophysin | rb | Abcam #ab14692 | colocalization in neurons with known synaptic vesicle markers, vendor validation immunofluorescence and western blot
SV2C | rb | Synaptic Systems #119202 | colocalization in neurons with known synaptic vesicle markers, vendor validation: western blot and immunofluorescence
4F2HC (CD98) | rb | polyclonal | Santa Cruz Biotech #sc9160 | morphology / subcellular localization, colocalization with LAT2
LAT2 (SLC7A8) | ms | monoclonal, clone #UMAB70 | OriGene #UM500058 | morphology / subcellular localization, colocalization with 4F2HC
Bestrophin 1 | rb | polyclonal | Abcam #ab14928 | vendor validation: immunofluorescence
GAT1 | rb | Synaptic Systems #274102 | vendor validation: immunofluorescence and western blot
GAT2 | rb | Abcam #ab2896 | vendor validation: immunofluorescence
GAT3 | rb | Synaptic Systems #274303 | vendor validation: western blot and immunofluorescence
GCP60 | rb | Novus Biologicals #NBP1-83379 | vendor validation: western blot in knockout cells and immunofluorescence
taurine | rb | Sigma-Aldrich #AB5022 | vendor validation: against a spectrum of antigens to assure hapten selectivity and proper affinity. No measurable glutaraldehyde-fixed tissue cross-reactivity (<1:1000) against L-alanine, γ-aminobutyrate, 1-amino-4-guanidobutane (AGB), D/L-arganine, D/L-aspartate, L-citrulline, L-cysteine, D/L-glutamate, D/L-glutamine, glutathione, glycine, L-lysine, L-ornithine, L-serine, L-threonine, L-tryptophan, L-tyrosine.

The following antibodies were utilized for Western blotting:

LRRC8A | rb | Cell Signaling #24979 | Western blotting: Band at expected molecular weight, knockout models show loss of expression, vendor validation: western blot
beta actin | ms | Sigma-Aldrich #A1978 | Western blotting: Single band at expected molecular weight, vendor validation: western blot, immunofluorescence, highly cited loading control antibody.

gp = guinea pig, ck = chicken, ms = mouse, rb = rabbit, sh = sheep

Eukaryotic cell lines

Policy information about cell lines

Cell line source(s)	GABA Biosensor CHO Cells (Novartis Institute for Biomedical Science) Serotonin Biosensor CHO Cells (Alejandro Caicedo lab, University of Miami) WT and LRRC8A-/- MIN6 cells (Rajan Sah lab, Washington University in St. Louis)
Authentication	Biosensor cells were authenticated in our labs to produce specific Ca2+ responses only to the intended ligand (see Methods section for extensive details). KO MIN6 cells were obtained at low passage and were authenticated by the generating lab (Rajan Sah, Univ. of Iowa) in a recent Nature Communications paper (doi:10.1038/s41467-017-02664-0).
Mycoplasma contamination	All cell lines tested negative for mycoplasma contamination
Commonly misidentified lines (See ICLAC register)	No commonly misidentified cell lines were used

Animals and other organisms

Policy information about studies involving animals; ARRIVE guidelines recommended for reporting animal research

Laboratory animals	Rat islets were isolated from pancreases of male and female P5 Sprague Dawley rats (Charles River). Mouse islets were isolated from the pancreases of 8-14 week old male and female LRRC8A-/- knockout mice and LRRC8A+/- heterozygous littermates.
Wild animals	The study did not involve wild animals.
Field-collected samples	The study did not involve samples collect from the field.
Ethics oversight	All experimental protocols using animals were approved by the University of Miami, University of Florida, or EPFL Animal Care and Use Committees.

Note that full information on the approval of the study protocol must also be provided in the manuscript.